Multi-dimensional Latent Group Structures with Heterogeneous Distributions

Xuan Leng[a] Heng Chen[b] Wendun Wang[c]

September 9, 2021

Abstract

This paper aims to identify the multi-dimensional latent grouped heterogeneity of distributional effects. We consider a panel quantile regression model with additive cross-section and time fixed effects. The cross-section effects and quantile slope coefficients are both characterized by grouped patterns of heterogeneity, but each unit can belong to different groups for cross-section effects and slopes. We propose a composite-quantile approach to jointly estimate multi-dimensional group memberships, slope coefficients, and fixed effects. We show that using multiple quantiles improves clustering accuracy if memberships are quantile-invariant. We apply the methods to examine the relationship between managerial incentives and risk-taking behavior.

Keywords: Composite quantile estimation, distributional heterogeneity, latent groups, panel quantile regressions, two-way fixed effects

JEL Classification: C31, C33, C38, G31, J33

[a]xleng@xmu.edu.cn. MOE Key Laboratory of Econometrics, Wang Yanan Institute for Studies in Economics, Department of Statistics and Data Science at School of Economics, and Fujian Key Lab of Statistics, Xiamen University, 422 Siming S Rd, Siming District, Xiamen, Fujian, China, 361005

[b]chhe@bankofcanada.ca. Currency Department, Bank of Canada, 234 Wellington St. W, Ottawa, ON K1A 0G9

[c]Corresponding author. wang@ese.eur.nl. Econometric Institute, Erasmus University Rotterdam and Tinbergen Institute, Burg. Oudlaan 50, 3062 PA Rotterdam, Netherlands

1 Introduction

The two-way fixed effects model has emerged as a common practice to analyze panel data in economics and finance as it allows researchers to control for unobserved heterogeneity in both cross-sectional and time-series dimensions. A salient empirical finding in panel data applications shows that the effect of covariates often exhibits a grouped pattern of heterogeneity, that is, homogeneous effects within a group (see, e.g., Mitton, 2002; Browning and Carro, 2007; Duchin et al., 2010, among many others), even when unobserved heterogeneity is accounted for. Hahn and Moon (2010) provided a theoretical foundation for group heterogeneity and Bonhomme et al. (2017) argued that group heterogeneity can be a good discrete approximation even if individual heterogeneity is present. Existing studies on panel group heterogeneity primarily focus on the (conditional) mean effects and cluster units based on the mean heterogeneity. However, in many applications, it is empirically useful to unveil the distributional effects of covariates and model the distributional heterogeneity (i.e., the difference in distributional effects across groups). For example, the impact of managerial incentives on R&D expenditure seems to vary across different levels of R&D expenditure, and such distributional effects may also vary across firms with distinct firm and managerial features. Hence, it is desirable for decision makers and investors to understand the heterogeneous distributional effects of managerial incentives on innovation-investment decisions. Moreover, it is crucial to control for unobserved cross-sectional and time heterogeneity in this study because investment decisions are obviously influenced by unobserved firm risk-taking strategies and various market events over the years.

This study presents a new model and estimation method to capture grouped patterns of distributional heterogeneity of covariate effects, while at the same time controlling for unobserved heterogeneity in both cross-sectional and time dimensions. We consider panel quantile regression models with additive cross-section and time fixed effects and allow the quantile slope coefficients to be group specific, such that units in the same group share common (conditional) distributional effects, while the distributions may differ across groups in the location, shape, or both. Moreover, the cross-section fixed effects are also characterized by a grouped pattern of heterogeneity in a similar spirit of Bonhomme and Manresa (2015a) and Gu and Volgushev (2019), but the associated group membership structure can differ from that of slope coefficients. In other words, each unit can belong to different groups for cross-section fixed effects and slope coefficients. The two group membership structures are both unknown, and we aim at identifying the two latent group structures (i.e., which units belongs to which group), leading to a multi-dimensional clustering problem. Modelling multi-dimensional group structures permits different degrees of heterogeneity in cross-section effects and slope coefficients, such that units in one group share a common coefficient vector but can differ in fixed effects, or vice versa. In contrast, one-dimensional clustering requires homogeneity of both cross-section effects and slopes within a group, and therefore cuts the data finer, rendering some groups with only a few units and of much smaller size than the others (also referred to as sparse interactions by Cheng et al. (2019); see also Cytrynbaum (2020) for related discussions). A small number of units in a group may lead to inaccurate or sometimes even infeasible estimation of group-specific parameters, especially when the

number of group-specific parameters is close or even larger than the number of observations in this group. Inaccurate estimation of group-specific parameters in turn deteriorates the clustering performance. Therefore, by imposing less strict requirements of homogeneity in a group, multi-dimensional clustering offers an effective and more flexible way of capturing cross-sectional heterogeneity than one-dimensional clustering. While our model and estimation approach allow group memberships to be dependent or common over quantiles, we focus on the latter case of quantile-invariant memberships, which is relevant in many empirical applications.[1] The quantile-invariant group structure allows us to pool information across quantiles to improve the group membership estimates.

We jointly estimate the multi-dimensional group memberships, slope coefficients, and fixed effects by minimizing a composite quantile check function, that is, a sum of the quantile check functions across different quantile levels over which the group structures are common. The composite quantile objective function allows us to utilize the information of group structures contained at multiple quantiles simultaneously and facilitates clustering. To solve the optimization problem, we employ an iterative algorithm that alters between group membership estimation and panel quantile regression estimation, similar in spirit to K-means clustering. In addition to establishing the consistency of membership and coefficient estimators, we comprehensively quantify the speed of convergence of the misclustering frequency (MF), a measure of clustering accuracy. We show that the speed of convergence is an exponential function of the length of time periods and that it depends on the number of quantiles used for clustering, degree of group separation, signal-to-noise ratio, and serial correlation of data. To the best of our knowledge, this is the first study that precisely quantifies how the clustering accuracy depends on the use of composite quantiles model and the features of data in the panel group structure literature.[2] We explicitly show that pooling information of multiple quantiles improves clustering accuracy if the group structure is invariant over these quantiles.

Our model is related with the burgeoning literature on panel structure models, for example, the K-means type of methods (Lin and Ng, 2012; Bonhomme and Manresa, 2015a; Liu et al., 2020; Ando and Bai, 2016; Vogt and Linton, 2016; Miao et al., 2020), Lasso-type of approaches (Su et al., 2016; Wang et al., 2018), pairwise comparisons (Krasnokutskaya et al., 2021), binary segmentation (Ke et al., 2016; Su and Wang, 2021), among others. More recently, Cheng et al. (2019) studied the multi-dimensional clustering in the presence of endogenous regressors. These methods cluster units based on the heterogeneity of conditional mean effects, while our work captures the grouped heterogeneity in the distributional effects. Sun (2005); Rosen et al. (2000); Ng and McLachlan (2014),

[1] In practice, group memberships are often driven by a few "inertial" factors that hardly vary across the distribution of the dependent variable. For example, Brand and Xie (2010) found that the economic returns of education differ significantly across individuals depending on how likely they are to attend college. Since the likelihood of attending college typically does not change over wage distribution, it seems plausible that the membership structure is also invariant to quantiles. Zwick and Mahon (2017) showed that firms' decisions to invest in equipment are affected by temporary tax incentives, and small firms respond far more actively to tax incentives than large firms do. Again, such underlying heterogeneity (size of a firm) varies little across the distribution of investment levels. The quantile-specific memberships can be easily incorporated in our estimation framework as will be clear in Section 2.2.

[2] Existing studies in the panel data classification literature only provide the consistency of the group membership estimates or show the convergence rate of the MF as an exponential function of the time-series dimension and some unknown number, such as Bonhomme and Manresa (2015a), Okui and Wang (2021), and Zhang et al. (2019a). They do not explain how data features influence clustering accuracy.

among others, considered a finite mixture of latent conditional distributions to model the distributional heterogeneity. These studies often assumed that the mixture probability depends on some observables or that the mixture distribution is composed of several known distributions. In contrast, we allow the group memberships and the distributions to be fully unrestricted. Another way of capturing the grouped pattern of distributional heterogeneity is to cluster units based on the empirical cumulative distribution function (CDF). Bonhomme et al. (2019) proposed to recover latent firm classes based on the empirical CDF of the earning distributions in an employer-employee matching study. Compared with empirical CDF-based clustering, regression quantiles may provide more detailed information on the distribution and thus stronger group separation, which further facilitates clustering.

This study also builds on a large amount of existing literature on panel quantile regression models. Following the seminal research of Koenker (2004), several influential studies have provided strict (asymptotic) analysis on the estimation and inference of panel quantile regressions with individual fixed effects, such as Galvao (2011), Kato et al. (2012), Galvao and Kato (2016) and Yoon and Galvao (2020), among many others. All these studies assume that the quantile regression coefficients are common across units. In contrast, we relax the cross-section homogeneity assumption and allow the quantile-specific coefficients to differ across units via a latent grouped pattern. Since our model contains time fixed effects, we need to deal with the incidental-parameter issue in the time dimension, in the similar spirit but symmetric to the existing studies that consider individual fixed effects. We show the consistency of the quantile slope estimates for each group, and use a similar idea as Galvao et al. (2020) to show the asymptotic normality of these estimates under a mild growth condition of the sample sizes. Chetverikov et al. (2016) considered a panel quantile regression with unit-specific slope coefficients, and model such heterogeneous slopes as a linear combination of a set of observed unit-level covariates. While allowing for a richer degree of heterogeneity than a group pattern, their model assumes a specific form of heterogeneity. If we regard those unit-level covariates as an indicator of the group memberships of units, this model can be viewed as a special case of panel quantile group structure models but with a known group membership structure. In contrast, we model the cross-sectional heterogeneity via *latent* and *unrestricted* group patterns, and we aim at identifying the latent group structures.

Two closely related works include Gu and Volgushev (2019) and Zhang et al. (2019a). Gu and Volgushev (2019) considered panel quantile regressions with grouped fixed effects and homogeneous slope coefficients, and cluster units based on a single quantile. We generalize their model by allowing time fixed effects and group heterogeneity in slopes. Moreover, when the group structure is invariant to quantiles, our composite-quantile estimation ensures that the estimated memberships are common over quantiles and also more accurate than those estimated using a single quantile. Zhang et al. (2019a) considered a panel quantile model allowing for group-specific slopes and individual-specific fixed effects. We differ from this work by considering both cross-section and time fixed effects and allowing for multi-dimensional group heterogeneity. Moreover, our asymptotic analysis complements Zhang et al. (2019a) by explicitly showing how the use of multiple quantiles influence clustering accuracy. While Zhang et al. (2019a) documented the advantages of the composite-quantile estimation via simulation, strict

theoretical justifications are missing.

We illustrate the economic importance of accounting for grouped heterogeneity in the distributional effects by revisiting the relationship between managerial incentives and risk-taking behavior measured by R&D expenditure. We find a significant degree of heterogeneity in the relationship between managerial incentives and risk-taking behavior across groups and across different locations of the conditional distribution of R&D expenditure. The grouped pattern is related with, yet sufficiently differs from industry grouping often imposed by applied finance researchers. The distributional heterogeneity and multi-dimensional latent groups in cross-section effects and slopes can be captured by our panel structure quantile regression models, but not by conventional linear panel regressions with two-way fixed effects.

The rest of the paper is organized as follows. Section 2 sets up the model and presents the estimation method given the number of groups. Section 3 provides the asymptotic properties of the proposed estimators. Section 4 discusses how to determine the number of groups. Section 5 presents the simulation study, and Section 6 discusses an empirical application. Section 7 concludes. The technical details are organized in the Supplementary Appendix.

2 Model setup and estimation

In this section, we first describe the setup of our model, and then explain the estimation approach.

2.1 Model setup

Suppose we observe $\{y_{it}, x_{it}\}_{i=1,\ldots,N,t=1,\ldots,T}$, where y_{it} is the scalar dependent variable of individual i observed at time t, and x_{it} is a $p \times 1$ vector of exogenous regressors. We are interested in the effect of x_{it} on the conditional quantile of y_{it}. Due to cross-sectional heterogeneity, the conditional quantile effect may vary across units (Galvao et al., 2017). We assume that the heterogeneous quantile effects can be characterized by a grouped pattern, such that units of the same group share a common conditional quantile effect. In addition, we allow for both cross-section and time fixed effects in the model, where the cross-section effects also exhibit a group pattern in a similar spirit of Gu and Volgushev (2019), while their group membership structure can differ from that of slope coefficients in an arbitrary manner. We write the model as

$$Q_\tau(y_{it}|x_{it}) = \alpha_{h_i}(\tau) + \lambda_t(\tau) + x_{it}'\beta_{g_i}(\tau), \quad i = 1, \ldots, N, \ t = 1, \ldots, T, \tag{2.1}$$

where $Q_\tau(y_{it}|x_{it})$ is the conditional τ-quantile of y_{it} given x_{it} with $\tau \in (0,1)$, $\alpha_{h_i}(\tau)$ and $\lambda_t(\tau)$ denote the cross-section and time fixed effects, and $\beta_{g_i}(\tau)$ is the group-specific quantile regression coefficient. The subscripts $h_i \in \{1, \ldots, H\}$ and $g_i \in \{1, \ldots, G\}$ denote the group memberships of unit i for cross-section fixed effects $\alpha(\tau)$ and slope coefficients $\beta(\tau)$, respectively, where $H < \infty$ and $G < \infty$ are the number of groups. Importantly, we allow the group structures of cross-section effects and slope coefficients both to be *latent*, which may depend on (possibly high-dimensional) observed and unob-

served covariates in an *unrestricted* manner. Such flexibility allows us to capture rich heterogeneity in a wide range of applications, even though G and H are assumed fixed and finite. Here we focus on the case where the group membership structure $\{h_i, g_i\}_{i=1}^N$ is time-invariant and independent of a range of quantiles, which is not an uncommon situation in practice. We refer to this model as multi-dimensional group structure quantile regressions (MuGS-QR).

Model (2.1) includes several important models as special cases. When $\tau = 0.5$, $h_i = g_i$ for all i, and there are no time fixed effects, our model collapses to a median regression with a single-level group structure of heterogeneity, which is closely related to the panel structure model with the group-specific conditional mean effects (Lin and Ng, 2012; Su et al., 2016). When the time fixed effects are absent and $\beta_{g_i}(\tau)$ is cross-sectionally homogeneous, our model reduces to the panel quantile grouped-specific fixed effects specification by Gu and Volgushev (2019), which extends the conditional mean grouped fixed effects (GFE) model of Bonhomme and Manresa (2015a). Since our model includes the time effects, we do face the incidental parameter problem as Zhang et al. (2019a) and Galvao et al. (2020) but in the time dimension, and some of our theoretical conditions are comparable to those of Galvao et al. (2020) by swapping the role of N and T. Our model can also be viewed as a quantile version of multi-dimensional clustering for panel mean regressions in Cheng et al. (2019), and we additionally allow for time effects but focus on exogenous regressors.

In model (2.1), we can identify the two latent group structures by using the time series of all units.[3] We discuss the group identifiability from the following two aspects. First, we can identify the latent group memberships for each individual if s/he has sufficient time observations lying in the non-overlapping region of the two groups. This is satisfied if one can observe each unit for infinitely many periods. Second, we allow the distribution of a group to be of any shape, including the multi-modal distribution, and can still correctly identify the group membership structures. Again, this is achieved by observing each unit for infinitely many periods. For example, if a group is characterized by a bimodal distribution, it would *not* be identified as two unimodal groups because the distribution of each unit in this group is bimodal.

2.2 Estimation method

There are two types of parameters in model (2.1): (i) the group membership variables $\{g_i\}_{i=1,\dots,N}$ and $\{h_i\}_{i=1,\dots,N}$ for the g-group and h-group structure, respectively; (ii) the regression quantile parameters $\beta_g(\tau) \in \mathbb{B}$, $\alpha_h(\tau) \in \mathbb{A}$, and $\lambda_t(\tau) \in \mathbb{D}$ for each fixed τ. Define $\boldsymbol{\beta}(\tau) := \{\beta_1'(\tau), \dots, \beta_G'(\tau)\}'$, $\boldsymbol{\alpha}(\tau) := \{\alpha_1(\tau), \dots, \alpha_H(\tau)\}'$, and $\boldsymbol{\lambda}(\tau) := \{\lambda_1(\tau), \dots, \lambda_T(\tau)\}'$. In practice, we consider a finite quantile sequence $\boldsymbol{\tau} := (\tau_1, \dots, \tau_K)'$, for which we denote $\boldsymbol{\beta}(\boldsymbol{\tau}) := \{\boldsymbol{\beta}'(\tau_1), \dots, \boldsymbol{\beta}'(\tau_K)\}'$, $\boldsymbol{\alpha}(\boldsymbol{\tau}) := \{\boldsymbol{\alpha}'(\tau_1), \dots, \boldsymbol{\alpha}'(\tau_K)\}'$, and $\boldsymbol{\lambda}(\boldsymbol{\tau}) := \{\boldsymbol{\lambda}'(\tau_1), \dots, \boldsymbol{\lambda}'(\tau_K)\}'$. We further collect these parameters as $\boldsymbol{\theta}(\boldsymbol{\tau}) = (\boldsymbol{\beta}(\boldsymbol{\tau}), \boldsymbol{\alpha}(\boldsymbol{\tau}), \boldsymbol{\lambda}(\boldsymbol{\tau})) \in \Theta$, where $\Theta = \mathbb{B}^{GK} \times \mathbb{A}^{HK} \times \mathbb{D}^{TK}$. For the membership parameters, denote $\gamma_g = \{g_1, \dots, g_N\} \in \Gamma_G$ and $\gamma_h = \{h_1, \dots, h_N\} \in \Gamma_H$ as the partition of N individuals into the G groups and H groups, respectively, where Γ_G and Γ_H denote the sets of all possible partitions. We

[3] This differs from group identification in the cross-sectional data, where the assumptions about the distribution of each group is typically required. See, for example, Dong and Lewbel (2011).

assume that both γ_g and γ_h are invariant to the quantile sequence $\boldsymbol{\tau}$. For the moment, we consider that the number of groups G and H are both finite and known. We shall discuss how to determine G and H in Section 4.

We propose to obtain the estimator of the two types of parameters, $\left(\widehat{\gamma}_g, \widehat{\gamma}_h, \widehat{\boldsymbol{\theta}}(\boldsymbol{\tau})\right)$, by minimizing the following composite quantile function

$$\min_{(\gamma_g,\gamma_h,\boldsymbol{\theta}(\boldsymbol{\tau}))\in\Gamma_G\times\Gamma_H\times\Theta} \frac{1}{NT}\sum_{i=1}^{N}\sum_{t=1}^{T}\sum_{k=1}^{K}\rho_{\tau_k}\left(y_{it}-\alpha_{h_i}(\tau_k)-\lambda_t(\tau_k)-x_{it}'\beta_{g_i}(\tau_k)\right), \tag{2.2}$$

where $\rho_\tau(u)=[\tau-I(u<0)]\,u$ is the check function. Typically, we consider K equally spaced quantiles, say, $\tau_k=k/(K+1)$ with $K\geq 1$.[4]

Our estimation method is related but significantly different from that of Zhang et al. (2019a), which considered one-way fixed effects and employed a two-step estimation approach by first removing fixed effects from the dependent variable using some preliminary consistent estimates, and then estimating the remaining parameters from a (composite) quantile check function with the transformed dependent variable (with fixed effects removed). Since we allow for both cross-section and time fixed effects, a preliminary consistent estimate of two-way fixed effects is not available without the knowledge of group memberships. Hence, we propose to jointly estimate group-related parameters along with the fixed effects. Moreover, we need to estimate the multi-dimensional group structures.

Since an exhaustive search of the optimal partition of the parameter space is virtually infeasible (Su et al., 2016), we solve the optimization problem in (2.2) via the following iterative algorithm:

Algorithm 1. *Let $\gamma_g^{(0)}$ and $\gamma_h^{(0)}$ be the initial estimate of γ_g and γ_h, respectively. Set $s=0$.*

Step 1 *For given $(\gamma_g^{(s)},\gamma_h^{(s)})$, estimate the regression quantile parameters for each τ_k as*

$$\boldsymbol{\theta}^{(s)}(\tau_k)=\underset{\boldsymbol{\theta}(\tau_k)\in\mathbb{B}^G\times\mathbb{A}^H\times\mathbb{D}^T}{\arg\min}\frac{1}{NT}\sum_{i=1}^{N}\sum_{t=1}^{T}\rho_{\tau_k}\left(y_{it}-\alpha_{h_i^{(s)}}(\tau_k)-\lambda_t(\tau_k)-x_{it}'\beta_{g_i^{(s)}}(\tau_k)\right),$$

for $k=1,\ldots,K$.

Step 2 *Given $\boldsymbol{\theta}^{(s)}(\boldsymbol{\tau})$ and $\gamma_h^{(s)}$, the g-group assignment for unit i is*

$$g_i^{(s+1)}=\underset{g\in\{1,\ldots,G\}}{\arg\min}\frac{1}{T}\sum_{t=1}^{T}\sum_{k=1}^{K}\rho_{\tau_k}\left(y_{it}-\alpha_{h_i^{(s)}}^{(s)}(\tau_k)-\lambda_t^{(s)}(\tau_k)-x_{it}'\beta_g^{(s)}(\tau_k)\right),$$

for $i=1,\ldots,N$.

[4]Our framework can be extended to allow the group structure to differ over quantiles. In fact, estimating quantile-specific group memberships can be regarded as a special case of our estimation procedure by applying (2.2) for each quantile separately.

Step 3 *Given* $\boldsymbol{\theta}^{(s)}(\boldsymbol{\tau})$ *and* $\gamma_g^{(s+1)}$*, the h-group assignment for unit* i *is*

$$h_i^{(s+1)} = \underset{h\in\{1,\ldots,H\}}{\arg\min} \frac{1}{T}\sum_{t=1}^{T}\sum_{k=1}^{K} \rho_{\tau_k}\left(y_{it} - \alpha_h^{(s)}(\tau_k) - \lambda_t^{(s)}(\tau_k) - x_{it}'\beta_{g_i^{(s+1)}}^{(s)}(\tau_k)\right),$$

for $i = 1, \ldots, N$.

Step 4 *Set* $s = s + 1$*. Go to Step 1 until numerical convergence of* $\boldsymbol{\theta}(\boldsymbol{\tau})$.

This algorithm iterates between the clustering and estimation steps. Step 1 estimates the quantile regression coefficients and fixed effects, given the group membership estimates. It applies the panel quantile regression estimation for each group. In Steps 2 and 3 (classification steps for two group structures), we update the group memberships based on the composite quantile check function, given the regression quantile estimates. These two steps contrast with the standard K-means (Lin and Ng, 2012; Bonhomme and Manresa, 2015a; Cheng et al., 2019) or Lasso-based (Su et al., 2016; Gu and Volgushev, 2019) algorithms that cluster units based only on the mean or a single quantile. Provided that the group memberships are common across the conditional distribution of the dependent variable, using multiple quantiles that contain clustering information, is expected to be more accurate in classification than the existing approaches. The more precise group membership estimates from Steps 2 and 3, in turn, improve the regression quantiles estimation in Step 1 in finite samples. The improvement by using multiple quantiles in clustering is especially significant when two groups are less well separated or when the signal-to-noise ratio is low. We formally study the effect of using multiple quantiles on the clustering accuracy in Section 3.

Like the K-means approach, this iterative algorithm depends on the initial values of group memberships. To avoid the local optimum, a typical solution is to try several different values and choose the one that associates with the minimum objective function. Another appealing choice of initial values would be the membership estimates obtained from a conditional mean regression, e.g., using the mean-based multi-dimensional clustering by Cheng et al. (2019). Given that group memberships are invariant to quantiles, the conditional mean regression provides a consistent, albeit likely inefficient, estimate of group memberships. This choice of initial values may avoid local optima and facilitate the convergence of the algorithm, at least to some extent.[5]

Remark 1. *Our setup of additive cross-section and time effects can be extended to time-varying grouped fixed effects (GFE), namely* $\alpha_{h_i,t}(\tau)$*, in the similar spirit as Bonhomme and Manresa (2015a). In this case, Algorithm 1 can still be applied, but the additive group and time dummies in the objective functions need to be replaced by their interactive dummies. Since we state the asymptotic properties of* $\alpha_{h_i}(\tau) + \lambda_t(\tau)$ *as a whole (see Theorem 1 and Corollary 1), our asymptotic analysis can be extended to allow for* $\alpha_{h_i,t}(\tau)$ *with some notational modifications.*

[5]Note that the minimum distance estimator as defined by Galvao et al. (2020) is difficult to implement in our model because neither unit-wise nor time-wise estimation is feasible due to the presence of cross-section and time fixed effects and latent group structures.

Remark 2. *Model (2.1) can also be extended to allow for different group patterns within the slope coefficient vector and to the case where a subvector of slope coefficients is homogeneous across units. Specifically, we can consider the model with multi-dimensional group patterns within the slope vector as*

$$Q_\tau(y_{it}|x_{it}) = \alpha_{h_i}(\tau) + \lambda_t(\tau) + x'_{(1),it}\beta_{(1),g_i}(\tau) + x'_{(2),it}\beta_{(2),l_i}(\tau),$$

where without loss of generality, we assume that the coefficients of the first p_1 explanatory variables $x_{(1),it}$ have coefficients $\beta_{(1),g_i}(\tau)$ indexed by the group membership variable $g_i \in \{1,\dots,G\}$, and the remaining variables $x_{(2),it}$ correspond to coefficients $\beta_{(2),l_i}(\tau)$ indexed by the membership variable $l_i \in \{1,\dots,L\}$, with the number of groups $G < \infty$ and $L < \infty$. In this model, $L = 1$ implies that the regressors $x_{(2),it}$ have homogeneous coefficients $\beta_{(2)}(\tau)$ for all i. Then, the objective function and the estimation algorithm can be correspondingly adjusted to incorporate the three-dimensional group heterogeneity or partial homogeneity.

3 Asymptotic properties

In this section, we study the asymptotic properties of the proposed estimators and demonstrate the advantages of using multiple quantiles for clustering. Through this section, we assume that the numbers of groups, G and H, are fixed and known. We use the superscript 0 to denote the true value, and let $\varepsilon_{it}(\tau) := y_{it} - Q^0_\tau(y_{it}|x_{it})$. For a vector v, $\|v\|$ denotes the usual Euclidean norm.

3.1 Weak consistency

We first show the consistency of quantile-specific slope coefficients and fixed effects. We impose the following conditions that assemble those of Kato et al. (2012) and Bonhomme and Manresa (2015a).

Assumption 1.

(*i*) The process $\{(y_{it} - \lambda^0_t(\tau), x_{it}), t \geq 1\}$ is strictly stationary for each unit i and $\tau \in (0,1)$, and independent across i.

(*ii*) There is some constant M such that $\sup_{i\geq 1}\|x_{i1}\| \leq M$ almost surely (a.s.).

(*iii*) Denote $F_{i,\tau}(u|x)$ as the conditional distribution of $\varepsilon_{i1}(\tau)$ given $x_{i1} = x$. For all $\delta > 0$,

$$\inf_{i\geq 1} \inf_{\sqrt{a^2+\|\boldsymbol{b}\|^2}=\delta} \mathsf{E}\left[\int_0^{a+x'_{i1}\boldsymbol{b}} (F_{i,\tau}(u|x_{i1}) - \tau)\, du\right] > 0.$$

(*iv*) For $h \in \{1,\dots,H\}$ and $g \in \{1,\dots,G\}$,

$$\lim_{N\to\infty} \frac{1}{N}\sum_{i=1}^N I\{h^0_i = h\} > 0 \quad \text{and} \quad \lim_{N\to\infty} \frac{1}{N}\sum_{i=1}^N I\{g^0_i = g\} > 0.$$

(v) For all $h \neq \widetilde{h}$ and $g \neq \widetilde{g}$, $\sum_{k=1}^{K} |\alpha_h^0(\tau_k) - \alpha_{\widetilde{h}}^0(\tau_k)| > 0$ and $\sum_{k=1}^{K} \|\beta_g^0(\tau_k) - \beta_{\widetilde{g}}^0(\tau_k)\| > 0$.

Assumption 1(i) requires that the time series of units remain stationary and are independent across units. Assumption 1(ii) imposes a uniform bound for the regressors over units. The same type of assumption is imposed in Kato et al. (2012, Assumption B1), Galvao and Kato (2016, Assumption A2), Zhang et al. (2019a, Assumption 1(c)) and Galvao et al. (2020, Condition (A1)). Assumption 1(iii) is an identification condition akin to A1(e) of Zhang et al. (2019a) and A3 of Kato et al. (2012) in the setup of panel quantile regressions with individual fixed effects. Assumption 1(iv) is identical to Assumption S(ii) in Cheng et al. (2019), which only requires sufficient units in each group for the two group structures, respectively; thus allowing for sparse interactions between any g-th and h-th groups, i.e., $\lim_{N\to\infty} \frac{1}{N} \sum_{i=1}^{N} I\{h_i^0 = h, g_i^0 = g\} = 0$ for some (h, g). Finally, Assumption 1(v) is the group separation condition that guarantees the identification of group-specific parameters subject to permutations of group labels. Note that it allows the groups to differ on at least one quantile index, for example, no separation at the mean but only at the tail quantile. Hence, our group separation condition is weaker than the standard mean-based separation condition (see, e.g., Bonhomme and Manresa, 2015a; Su et al., 2016; Cheng et al., 2019).

Theorem 1. *Under Assumptions 1(i)–1(iii), if* $\log T/N \to 0$ *as* N *and* $T \to \infty$, *for* $k = 1, \ldots, K$, *we have that*

$$\max_{i=1,\ldots,N} \left\| \widehat{\beta}_{\widehat{g}_i}(\tau_k) - \beta_{g_i^0}^0(\tau_k) \right\| \xrightarrow{\mathsf{P}} 0, \tag{3.1}$$

and

$$\max_{i=1,\ldots,N} \left| \widehat{\alpha}_{\widehat{h}_i}(\tau_k) + \widehat{\lambda}_t(\tau_k) - (\alpha_{h_i^0}^0(\tau_k) + \lambda_t^0(\tau_k)) \right| \xrightarrow{\mathsf{P}} 0 \tag{3.2}$$

for $t = 1, \ldots, T$.

This theorem establishes the consistency of regression quantile estimators under the estimated group memberships uniformly across units. Note that we require large N, namely $\log T/N \to 0$, to achieve the consistency. This growth condition of the sample sizes is "symmetric" to the condition $\log N/T \to 0$ imposed by Kato et al. (2012) and Zhang et al. (2019a), because model (2.1) contains incidental parameters in the time (but not the cross-sectional) dimension. While this theorem states the convergence of parameter estimates at each quantile τ_k, the arguments can be extended uniformly over the quantiles, provided that the number of quantiles for estimation is finite.

As the objective function is invariant to the relabeling of groups, we can profile out the group memberships and obtain the consistency for the group-specific parameters. The following corollary establishes the convergence of quantile estimators uniformly for all groups.

Corollary 1. *Under Assumption 1, if* $\log T/N \to 0$ *as* N *and* $T \to \infty$, *for* $k = 1, \ldots, K$, *we have that*

$$\max_{g\in\{1,\ldots,G\}} \left\| \widehat{\beta}_g(\tau_k) - \beta_g^0(\tau_k) \right\| \xrightarrow{\mathsf{P}} 0, \tag{3.3}$$

and

$$\max_{h\in\{1,\ldots,H\}}\max_{1\le t\le T}\left|\widehat{\alpha}_h(\tau_k)+\widehat{\lambda}_t(\tau_k)-(\alpha_h^0(\tau_k)+\lambda_t^0(\tau_k))\right|\xrightarrow{\mathsf{P}}0, \tag{3.4}$$

provided that $G<\infty$ *and* $H<\infty$.

3.2 Asymptotic behavior of misclustering frequency

In this section, we examine the accuracy of the group membership estimates via the misclustering frequency, a widely used measure of clustering accuracy. We investigate how the use of distributional information and other features of data affect the accuracy. The misclustering frequency for the two-dimensional group structures is given by

$$\text{MF}=1-\frac{1}{N}\sum_{i=1}^{N}I\{\widehat{g}_i=g_i^0,\widehat{h}_i=h_i^0\}.$$

Since the value of MF depends on permutations of group labeling, the theoretical properties discussed below hold under a suitable choice of labeling. Before analyzing the general case of model (2.1), we illustrate the intuition and show the behavior of MF in a simple example.

Illustrative example: To facilitate the presentation, we focus on one-dimensional clustering in the following regression model without covariates:

$$y_{it}=\beta_{g_i}+\varepsilon_{it},\quad g_i\in\{1,2\}, \tag{3.5}$$

where the intercept is characterized by two groups ($G=2$), and ε_{it} follows $N(0,\sigma_\varepsilon^2)$ and is independently and identically distributed (i.i.d.) across t for each i. We show how the use of composite quantiles and the features of data affect the behavior of misclustering probability $\mathsf{P}(\widehat{g}_i\neq g_i^0)$ by deriving the rate at which $\mathsf{P}(\widehat{g}_i\neq g_i^0)$ converging to 0 as T tends to infinity.[6] Denote q_τ as the $100\tau\%$ quantile of $N(0,\sigma_\varepsilon^2)$. Note that $Q_\tau(y_{it})=\beta_{g_i}+q_\tau=:\beta_{g_i}(\tau)$. Define $W_{it,g}(\boldsymbol{\beta}(\boldsymbol{\tau})):=\sum_{k=1}^K\{\rho_{\tau_k}(y_{it}-\beta_g(\tau_k))-\rho_{\tau_k}(y_{it}-\beta_{g_i^0}(\tau_k))\}$. For any $g\neq g_i^0$, conditional on the slope estimator $\widehat{\boldsymbol{\beta}}(\boldsymbol{\tau})$, we have

$$\begin{aligned}\mathsf{P}\big(\widehat{g}_i\neq g_i^0\big)&=\sum_{g\neq g_i^0}\mathsf{P}\big(\widehat{g}_i=g\big)\\&\le\sum_{g\neq g_i^0}\mathsf{P}\bigg(T^{-1}\sum_{t=1}^{T}W_{it,g}(\widehat{\boldsymbol{\beta}}(\boldsymbol{\tau}))\le 0\bigg)\\&=O\bigg(T^{-1/2}\sum_{g\neq g_i^0}\exp\bigg(-T\frac{\mathsf{E}^2[W_{i1,g}(\widehat{\boldsymbol{\beta}}(\boldsymbol{\tau}))]}{2\mathsf{Var}\left[W_{i1,g}(\widehat{\boldsymbol{\beta}}(\boldsymbol{\tau}))\right]}\bigg)\bigg),\end{aligned}$$

[6] Strictly speaking, $\mathsf{P}(\widehat{g}_i=g_i)$ is a conditional probability since $\widehat{g}_i$ depends on $\widehat{\boldsymbol{\beta}}(\boldsymbol{\tau})$.

where the mean and variance of $W_{i1,g}(\widehat{\boldsymbol{\beta}}(\boldsymbol{\tau}))$ can be obtained, respectively, as

$$\mathsf{E}[W_{i1,g}(\widehat{\boldsymbol{\beta}}(\boldsymbol{\tau}))] = \sum_{k=1}^{K} \int_0^{\beta_g^0 - \beta_{g_i^0}^0} \left\{ \Phi\left(\frac{u + q_{\tau_k}}{\sigma_\varepsilon} \right) - \tau_k \right\} du + o_{\mathsf{P}}(1),$$

and

$$\begin{aligned} &\mathsf{Var}\left[W_{i1,g}(\widehat{\boldsymbol{\beta}}(\boldsymbol{\tau}))\right] \\ &= \sum_{k=1}^{K} \sum_{l=1}^{K} \int_0^{\beta_g^0 - \beta_{g_i^0}^0} \int_0^{\beta_g^0 - \beta_{g_i^0}^0} \left\{ \Phi\left(\frac{(u + q_{\tau_k}) \wedge (s + q_{\tau_l})}{\sigma_\varepsilon} \right) - \Phi\left(\frac{u + q_{\tau_k}}{\sigma_\varepsilon} \right) \Phi\left(\frac{s + q_{\tau_l}}{\sigma_\varepsilon} \right) \right\} du ds + o_{\mathsf{P}}(1). \end{aligned}$$

The derivations and more detailed discussions can be found in the Supplementary Appendix. The above results show that the misclustering probability depends on the number of used quantiles for clustering (K), the degree of group separation ($\beta_g^0 - \beta_{g_i^0}^0$ for $g \neq g_i^0$), and the standard deviation of the error term (σ_ε). To better demonstrate such dependence, we plot the misclustering probability with $g_i^0 = 1$, as we vary K, $\beta_2^0 - \beta_1^0$, and σ_ε in Figure 1.

Figure 1: misclustering probability in the illustrative example

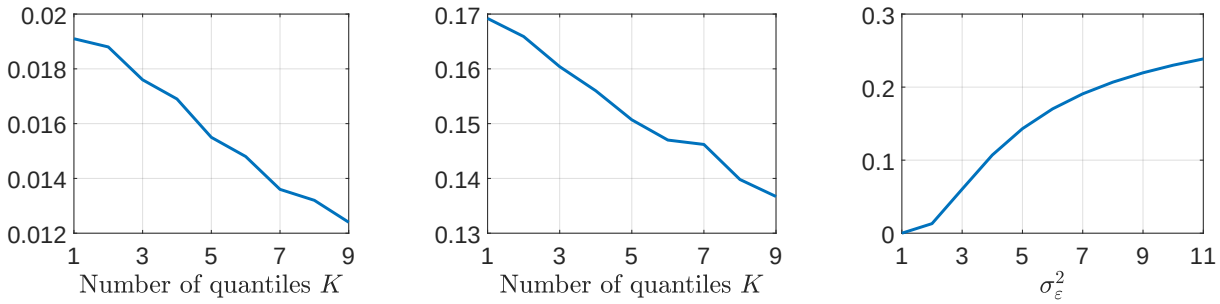

(a) $\beta_2^0 - \beta_1^0 = 1, \sigma_\varepsilon^2 = 1$ (b) $\beta_2^0 - \beta_1^0 = 0.5, \sigma_\varepsilon^2 = 1$ (c) $\beta_2^0 - \beta_1^0 = 1, K = 9$

The left panel of Figure 1 fixes $\beta_2^0 - \beta_1^0 = 1$ and $\sigma_\varepsilon^2 = 1$, but varies the number of quantiles used for estimation. It shows that the misclustering probability is a decreasing function on K, implying that using multiple quantiles does improve clustering accuracy. The middle panel considers a smaller degree of group separation, i.e., $\beta_2^0 - \beta_1^0 = 0.5$, while we see a larger misclustering probability than the left panel. The right panel suggests, as expected, that an increase of σ_ε leads to a larger misclustering probability. ∎

Next, we study the asymptotic property of MF in the general setup as in model (2.1). For all $\delta > 0$, define the neighborhood of the true values of parameters as

$$\begin{aligned} \mathbb{N}_\delta := \big\{ \boldsymbol{\theta}(\boldsymbol{\tau}) \in \Theta : &\max_{g \in \{1,\ldots,G\}} \|\beta_g(\tau_k) - \beta_g^0(\tau_k)\| < \delta, \\ &\max_{h \in \{1,\ldots,H\}} \max_{1 \le t \le T} \left| \alpha_h(\tau_k) + \lambda_t(\tau_k) - (\alpha_h^0(\tau_k) + \lambda_t^0(\tau_k)) \right| < \delta, \forall k = 1, \ldots, K \big\}. \end{aligned} \tag{3.6}$$

From Corollary 1, $\widehat{\boldsymbol{\theta}}(\boldsymbol{\tau}) \in \mathbb{N}_\delta$ when N and T are large. Conditional on $\boldsymbol{\theta}(\boldsymbol{\tau}) \in \mathbb{N}_\delta$, we investigate the rate at which MF converges to 0. To this end, we introduce the mixing conditions of the strictly stationary processes $\{(y_{it} - \lambda_t^0(\tau), x_{it}), t \geq 1\}$ for $i = 1, \ldots, N$. Let S be a subset of $\{1, \ldots, T\}$ and denote $\sigma\big((y_{it} - \lambda_t^0(\tau), x_{it}), t \in S\big)$ as the sub σ-field generated from $\{(y_{it} - \lambda_t^0(\tau), x_{it}), t \in S\}$ on the measurable space $(\Omega, \mathcal{A})$. For any positive integer m, define the strong and ρ-mixing coefficients of each process as

$$\alpha_i(m, T) = \sup_{n \in \mathbb{Z}^+} \alpha\left(\sigma\left((y_{it} - \lambda_t^0(\tau), x_{it}), 1 \leq t \leq n\right), \sigma\left((y_{it} - \lambda_t^0(\tau), x_{it}), n + m \leq t \leq T\right)\right),$$

and

$$\rho_i^*(m, T) = \sup_{\substack{\forall S_1, S_2 \subset \{1, \ldots, T\} \\ \min_{t_1 \in S_1, t_2 \in S_2} |t_1 - t_2| \geq m}} \rho\left(\sigma\left((y_{it} - \lambda_t^0(\tau), x_{it}), t \in S_1\right), \sigma\left((y_{it} - \lambda_t^0(\tau), x_{it}), t \in S_2\right)\right),$$

where $\alpha(\cdot, \cdot)$ and $\rho(\cdot, \cdot)$ are the measures of serial dependence applied to any two sub σ-fields of $\mathcal{A}$.[7]

Assumption 2.

(i) Denote $\alpha(m) := \sup_{i \geq 1} \lim_{T \to \infty} \alpha_i(m, T)$ and $\rho^*(m) := \sup_{i \geq 1} \lim_{T \to \infty} \rho_i^*(m, T)$. Assume that $\alpha(m) \to 0$ as $m \to \infty$ and $\rho^*(1) \in [0, 1)$.

(ii) For each unit i, define

$$W_{it,gh}(\boldsymbol{\theta}(\boldsymbol{\tau})) = \sum_{k=1}^{K} \left\{\rho_{\tau_k}\left(y_{it} - \alpha_h(\tau_k) - \lambda_t(\tau_k) - x_{it}'\beta_g(\tau_k)\right) - \rho_{\tau_k}\left(y_{it} - \alpha_{h_i^0}(\tau_k) - \lambda_t(\tau_k) - x_{it}'\beta_{g_i^0}(\tau_k)\right)\right\}.$$

If the process $\{W_{it,gh}(\boldsymbol{\theta}^0(\boldsymbol{\tau})), t \geq 1\}$, with $\boldsymbol{\theta}^0(\boldsymbol{\tau})$ denoting the true value of $\boldsymbol{\theta}(\boldsymbol{\tau})$, admits the central limit theorem (CLT), then the following uniform convergence holds:

$$\lim_{T \to \infty} \sup_{x \in \mathbb{R}} \left| \mathsf{P}\left(\sqrt{T} \, \frac{T^{-1} \sum_{t=1}^{T} W_{it,gh}(\boldsymbol{\theta}^0(\boldsymbol{\tau})) - \mathsf{E}[W_{i1,gh}(\boldsymbol{\theta}^0(\boldsymbol{\tau}))]}{\sqrt{\mathsf{Var}\left[W_{i1,gh}(\boldsymbol{\theta}^0(\boldsymbol{\tau}))\right]}} \leq x \right) - \Phi(x) \right| = 0,$$

where Φ is the standard normal distribution function, and the mean and variance of $W_{i1,gh}(\boldsymbol{\theta}^0(\boldsymbol{\tau}))$ are given by (A.23) and (A.28), respectively, in the Supplementary Appendix.

Assumption 2(i) requires that the process $\{(y_{it} - \lambda_t^0(\tau), x_{it}), t \geq 1\}$ is strongly mixing for each unit. Moreover, $\rho^*(1) < 1$ assures that $\sup_{i \geq 1} T^{-1} \mathsf{Var}\left[\sum_{t=1}^{T} W_{it,gh}(\boldsymbol{\theta}^0(\boldsymbol{\tau}))\right] < \infty$ which is needed for the CLT of each process $\{W_{it,gh}(\boldsymbol{\theta}^0(\boldsymbol{\tau})), t \geq 1\}$. Assumption 2$(ii)$ strengthens pointwise convergence to uniform convergence of the CLT, which is used to quantify the order of rate for MF (see (A.27) in the Supplementary Appendix). When the process $\{(y_{it} - \lambda_t^0(\tau), x_{it}), t \geq 1\}$ is independent across t, Assumption 2(ii) holds due to Berry-Esseen theorem (see Feller, 1991).

[7] Let $\mathcal{A}_1$ and $\mathcal{A}_2$ be any two sub σ-fields of $\mathcal{A}$. The two dependence measures are given by $\alpha(\mathcal{A}_1, \mathcal{A}_2) = \sup_{A_1 \in \mathcal{A}_1, A_2 \in \mathcal{A}_2} |\mathsf{P}(A_1 \cap A_2) - \mathsf{P}(A_1)\mathsf{P}(A_2)|$, and $\rho(\mathcal{A}_1, \mathcal{A}_2) = \sup_{f \in \mathcal{L}^2(\mathcal{A}_1), h \in \mathcal{L}^2(\mathcal{A}_2)} |\mathsf{E}fh - \mathsf{E}f\mathsf{E}h| / \sqrt{\mathsf{E}f^2 \mathsf{E}h^2}$, where $\mathcal{L}^2(\mathcal{A})$ denotes the space of square-integrable and $\mathcal{A}$-measurable random variables.

The following theorem depicts the rate of convergence for MF.

Theorem 2. *Suppose Assumptions 1–2 hold and* $\log T/N \to 0$. *For any* $0 < \epsilon < 1$, *there exists* δ *such that conditional on* $\boldsymbol{\theta}(\boldsymbol{\tau}) \in \mathbb{N}_\delta$, *as* N *and* $T \to \infty$,

$$\sup_{\boldsymbol{\theta}(\boldsymbol{\tau})\in\mathbb{N}_\delta} 1 - \frac{1}{N}\sum_{i=1}^{N} I\{\widehat{g}_i = g_i^0, \widehat{h}_i = h_i^0\} = O_{\mathsf{P}}\left(\frac{\exp(-T\zeta/2)}{N^{1/2}T^{1/4}} + \frac{\exp(-T\zeta)}{T^{1/2}}\right), \tag{3.7}$$

where

$$\zeta = \frac{(1-\epsilon)^2}{2} \cdot \frac{1-\rho^*(1)}{1+\rho^*(1)} \cdot \frac{\inf_{i\geq 1} \min_{(g,h)\neq(g_i,h_i)} \mathsf{E}^2[W_{i1,gh}(\boldsymbol{\theta}^0(\boldsymbol{\tau}))]}{\sup_{i\geq 1} \max_{(g,h)} \mathsf{Var}\left[W_{i1,gh}(\boldsymbol{\theta}^0(\boldsymbol{\tau}))\right]} > 0.$$

This theorem shows that the MF converges to zero as N and T increase with the rate shown in (3.7). The first term, $O_{\mathsf{P}}\left(\frac{\exp(-T\zeta/2)}{N^{1/2}T^{1/4}}\right)$, controls the rate when $T^{1/2}\exp(T\zeta)$ grows faster than N. Otherwise, the second term, $O_{\mathsf{P}}\left(\frac{\exp(-T\zeta)}{T^{1/2}}\right)$, dominates in the rate. The exponential decrease of T on the clustering accuracy is consistent with Bonhomme and Manresa (2015a) and Okui and Wang (2021), both of which show the clustering accuracy improving exponentially as T increases. It also complements Lemma 3 in Zhang et al. (2019b) by explicitly quantifying how multiple quantiles and features of data influence the clustering accuracy. This theorem shows that the accuracy of clustering is affected by the serial dependence of data (measured by $\rho^*(1)$), magnitude of the noise, number of quantiles used for the estimation, and degree of group separation, the latter three of which appear in the moments of $W_{i1,gh}(\boldsymbol{\theta}^0(\boldsymbol{\tau}))$. More particularly, a strong serial dependence in data and a large variance of errors impede the rate of convergence for MF, while more quantiles used for estimation and a large degree of group separation can improve the rate.

Remark 3. *The potential improvement by using multiple quantiles is, of course, conditional on a common group structure across multiple quantiles. If certain quantiles contain no information for clustering, incorporating these "uninformative" quantiles may lead to lower clustering accuracy than using the most informative quantile (see also Zhang et al., 2019a). However, in practice, it is difficult to identify the best single quantile that contains the strongest signal of clustering; therefore, the composite-quantile-based clustering offers a robust approach that works effectively, provided that the clustering signals across quantiles do not conflict.*

The next corollary is an immediate result from Theorem 2.

Corollary 2. *Under the conditions of Theorem 2, if* $N/(T^{1/2}\exp(T\epsilon)) \to 0$ *for all* $\epsilon > 0$, *we obtain*

$$\mathsf{P}\left(\bigcup_{i=1}^{N}\{(\widehat{g}_i, \widehat{h}_i) \neq (g_i^0, h_i^0)\}\right) \to 0$$

as N *and* $T \to \infty$, *where* $\bigcup$ *denotes the union of events.*

This corollary states the consistency of group membership estimates uniformly across all units. Note that in addition to $\log T/N \to 0$, we require an additional growth condition of sample sizes, namely $N/(T^{1/2}\exp(T\epsilon)) \to 0$ for all $\epsilon > 0$. This condition holds when N grows polynomially in T.

3.3 Asymptotic distribution

Finally, we derive the asymptotic distribution of the group-specific slope coefficient estimates. First, we show the asymptotic equivalence between the estimates obtained under the unknown and true group memberships. Let $\widetilde{\boldsymbol{\theta}}(\boldsymbol{\tau}) = \big(\widetilde{\boldsymbol{\beta}}(\boldsymbol{\tau}), \widetilde{\boldsymbol{\alpha}}(\boldsymbol{\tau}), \widetilde{\boldsymbol{\lambda}}(\boldsymbol{\tau})\big)$ denote the vector of the estimated slope coefficient and fixed effects under the true group structure. It is obtained by

$$\widetilde{\boldsymbol{\theta}}(\boldsymbol{\tau}) = \underset{\boldsymbol{\theta}(\boldsymbol{\tau})\in\Theta}{\arg\min} \ \frac{1}{NT}\sum_{i=1}^{N}\sum_{t=1}^{T}\sum_{k=1}^{K}\rho_{\tau_k}\left(y_{it} - \alpha_{h_i^0}(\tau_k) - \lambda_t(\tau_k) - x_{it}'\beta_{g_i^0}(\tau_k)\right). \tag{3.8}$$

To examine the impact of error caused by estimating latent group structures on the slope estimates, an extra assumption is imposed.

Assumption 3. Let $\omega_{t,\tau_k}(h,g)$ denote the minimum eigenvalue of the following matrix:

$$\frac{1}{N}\sum_{i:h_i^0=h,g_i^0=g}\mathsf{E}\left[f_{i,\tau_k}\left(\alpha_h(\tau_k)+\lambda_t(\tau_k)-\big(\alpha_h^0(\tau_k)+\lambda_t^0(\tau_k)\big)+x_{it}'\big(\beta_g(\tau_k)-\beta_g^0(\tau_k)\big)|x_{it}\right)\left(1,x_{it}'\right)'\left(1,x_{it}'\right)\right],$$

where $h\in\{1,\ldots,H\}$ and $g\in\{1,\ldots,G\}$. Conditional on $\boldsymbol{\theta}(\boldsymbol{\tau})\in\mathbb{N}_\delta$ with some $\delta>0$,

$$\inf_{\boldsymbol{\theta}(\boldsymbol{\tau})\in\mathbb{N}_\delta}\inf_{t\geq 1}\omega_{t,\tau_k}(h,g)\to\underline{\omega}_{\tau_k}(h,g)>0, \quad \text{and} \quad \sup_{\boldsymbol{\theta}(\boldsymbol{\tau})\in\mathbb{N}_\delta}\sup_{t\geq 1}\omega_{t,\tau_k}(h,g)\to\overline{\omega}_{\tau_k}(h,g)<\infty,$$

for $k=1,\ldots,K$.

Assumption 3 is a full rank condition, which is comparable to Assumption 1(f) in Zhang et al. (2019a). The following corollary relates the slope coefficient estimates obtained from the unknown and true multi-dimensional group memberships.

Corollary 3. *Suppose Assumptions 1–3 hold. For $k=1,\ldots,K$, we have*

$$\max_{g\in\{1,\ldots,G\}}\|\widehat{\beta}_g(\tau_k)-\widetilde{\beta}_g(\tau_k)\|^2 = O_{\mathsf{P}}\left(\frac{\exp(-T\zeta/2)}{N^{1/2}T^{1/4}}+\frac{\exp(-T\zeta)}{T^{1/2}}\right), \tag{3.9}$$

as N and $T\to\infty$, where ζ is defined in Theorem 2.

This corollary states that the estimator of slope coefficients under the unknown (and estimated) multi-dimensional group memberships converge to the infeasible estimator obtained under the true memberships at an exponential rate of T, which further implies that the impact of the clustering error on the coefficient estimates is limited. With the asymptotic equivalence, we can obtain the asymptotic distribution of $\widehat{\beta}_g(\tau_k)$ by studying that of $\widetilde{\beta}_g(\tau_k)$ for each $g\in\{1,\ldots,G\}$. We show the Bahadur representation and asymptotic normality of $\widetilde{\beta}_g(\tau_k)$. Recall that $\varepsilon_{it}(\tau_k)=y_{it}-Q_{\tau_k}^0(y_{it}|x_{it})$ and $F_{i,\tau_k}(u|x)$ is the conditional distribution of $\varepsilon_{i1}(\tau_k)$ given $x_{i1}=x$. We add extra regularity conditions as follows.

Assumption 4.

(*i*) For each fixed i, the observations $\{(y_{it}, x_{it}), t \geq 1\}$ are independent across t.

(*ii*) Let $I_g := \{i : g_i^0 = g\}$. For each t, $\{(y_{it} - \alpha_{h_i^0}^0(\tau_k), x_{it}), i \in I_g\}$ are identically distributed across i.

(*iii*) For each i, the eigenvalues of $\mathsf{E}[(1, x_{i1}')'(1, x_{i1}')]$ are bounded away from zero and infinity.

(*iv*) For each i, $F_{i,\tau_k}(u|x)$ is twice differentiable with respect to u for all x, and denote $f_{i,\tau_k}(u|x) := \partial F_{i,\tau_k}(u|x)/\partial u$ and $f'_{i,\tau_k}(u|x) := \partial f_{i,\tau_k}(u|x)/\partial u$. The following inequalities hold:

$$\overline{c}_f := \sup_{(u,x)} f_{i,\tau_k}(u|x) < \infty \quad \text{and} \quad \sup_{(u,x)} |f'_{i,\tau_k}(u|x)| < \infty.$$

(*v*) There exists some constant $\underline{c}_f < \overline{c}_f$ such that

$$0 < \underline{c}_f \leq \inf_t \inf_{\tau \in \mathcal{T}_k} \inf_x f_{i,\tau_k}\big(\alpha_{h_i^0}^0(\tau) + \lambda_t^0(\tau) - \big(\alpha_{h_i^0}^0(\tau_k) + \lambda_t^0(\tau_k)\big) + x'\big(\beta_{g_i^0}^0(\tau) - \beta_{g_i^0}^0(\tau_k)\big)|x\big),$$

where $\mathcal{T}_k$ denotes an open neighborhood of τ_k.

(*vi*) For all $h \in \{1, \ldots, H\}$ and $g \in \{1, \ldots, G\}$, $\lim_{N\to\infty} N^{-1} \sum_{i=1}^N I\{h_i^0 = h, g_i^0 = g\} > 0$.

(*vii*) Let $\iota_{h,g} := \sum_{i:h_i^0=h,g_i^0=g} \mathsf{E}[f_{i,\tau_k}(0|x_{i1})x_{i1}] / \sum_{i:h_i^0=h,g_i^0=g} f_{i,\tau_k}(0)$, and define

$$\Gamma_{Ng} := \frac{1}{N} \sum_{h\in\{1,\ldots,H\}} \sum_{i:h_i^0=h,g_i^0=g} \mathsf{E}[f_{i,\tau_k}(0|x_{i1})x_{i1}(x_{i1}' - \iota_{h,g}')].$$

Assume that Γ_{Ng} is nonsingular for each N, and $\Gamma_g := \lim_{N\to\infty} \Gamma_{Ng}$ exists and is nonsingular. Moreover, the limit $V_g := \lim_{N\to\infty} N^{-1} \sum_{h\in\{1,\ldots,H\}} \sum_{i:h_i^0=h,g_i^0=g} \mathsf{E}[(x_{i1} - \iota_{h,g})(x_{i1} - \iota_{h,g})']$ exists and is nonsingular.

Assumption 4(*i*), in combination with Assumption 1(*i*), implies that $\{(y_{it}, x_{it})\}$ are independent across t for all i. This is needed to apply the proving strategy of Volgushev et al. (2019), such that the variance of the remainder term of $\widetilde{\beta}_g(\tau_k) - \beta_g^0(\tau_k)$ is controlled (see the second term on the right side of (A.49)).[8] Assumption 4(*ii*) requires that units from each group g are i.i.d. to make use of some standard probability inequalities. Assumptions 4(*iii*)–4(*v*) resemble Conditions (A1)–(A3) in Galvao et al. (2020), but are adjusted to account for multi-dimensional group structures and time fixed effects. Assumption 4(*vi*) assures sufficient units in the interaction of any g and h groups, such that the pooled estimate of $\alpha_h(\tau_k) + \lambda_t(\tau_k)$ using these units, defined as

$$\alpha_h^*(\tau_k) + \lambda_t^*(\tau_k) := \underset{(\alpha,\lambda)\in\mathbb{A}\times\mathbb{D}}{\arg\min} \sum_{i:h_i^0=h,g_i^0=g} \rho_{\tau_k}\left(y_{it} - (\alpha + \lambda) - x_{it}'\beta_g^0(\tau_k)\right),$$

[8] Since the remainder term of the representation of $\widetilde{\beta}_g(\tau_k) - \beta_g^0(\tau_k)$ sums across t due to the presence of time fixed effects, it is difficult to allow for the dependence across t in the asymptotic analysis here as in Galvao et al. (2020). As our focus is mainly on the multi-dimensional clustering, we leave the analysis of asymptotic distribution in the dependent case as future research.

is sufficiently close to $\alpha_h^0(\tau_k) + \lambda_t^0(\tau_k)$. This condition is stronger than Assumption 1(*iv*) and needed here since we follow the proving strategy of Galvao et al. (2020) to relax the growth condition of sample sizes for asymptotic normality (see Remark 3 therein), where $\alpha_h^*(\tau_k) + \lambda_t^*(\tau_k)$ is used to approximate the remainder term of $\widetilde{\beta}_g(\tau_k) - \beta_g^0(\tau_k)$. We can relax this assumption at the cost of a stronger growth condition of sample sizes (see the growth condition in Theorem 3.2 of Kato et al., 2012) in a symmetric sense. Assumption 4(*vii*) guarantees the existence of the quantities needed for the asymptotic covariance matrix of $\widetilde{\beta}_g(\tau_k)$, and is standard in the literature of panel quantile regression (see, e.g., Condition (B3) in Kato et al., 2012).

Lemma 1. *Suppose Assumptions 1 and 4 hold. If* $\log T/N \to 0$ *and* N *grows at most polynomially in* T*, then for each group* g*,* $\widetilde{\beta}_g(\tau_k)$ *admits the following expansion:*

$$\begin{aligned}
&\widetilde{\beta}_g(\tau_k) - \beta_g^0(\tau_k) + o_{\mathsf{P}}(\|\widetilde{\beta}_g(\tau_k) - \beta_g^0(\tau_k)\|) \\
&= \Gamma_{Ng}^{-1}\left[\frac{1}{NT}\sum_{t=1}^{T}\sum_{h\in\{1,\ldots,H\}}\sum_{i:h_i^0=h,g_i^0=g}\{\tau_k - I(\varepsilon_{it}(\tau_k)\le 0)\}(x_{it}-\iota_{h,g})\right] \\
&\quad + O_{\mathsf{P}}\big(N^{-3/4}T^{-1/4}(\log N)^{1/2} + N^{-1}\log N\big). \qquad (3.10)
\end{aligned}$$

Moreover, if $T(\log N)^2/N \to 0$*, then we have*

$$\sqrt{NT}(\widetilde{\beta}_g(\tau_k) - \beta_g^0(\tau_k)) \xrightarrow{D} \mathbb{N}(\mathbf{0}, \tau_k(1-\tau_k)\Gamma_g^{-1}V_g\Gamma_g^{-1}),$$

as N *and* $T \to \infty$*.*

The results in Lemma 1 are comparable to Theorem 1 of Galvao et al. (2020) for panel quantile regressions with individual effects. As (3.8) includes the incidental parameters in the time instead of the cross-sectional dimension, our growth condition of the sample sizes for asymptotic normality, namely $T(\log N)^2/N \to 0$, is symmetric to that of Galvao et al. (2020) by swapping the role of N and T, and is weaker compared with those imposed in the literature of panel quantile regressions with group heterogeneity. For example, Zhang et al. (2019a) require a much larger T than N to achieve asymptotic normality, namely $N^2(\log N)^3/T \to 0$, which is a much stronger condition in the symmetric sense. Here the restriction of the polynomial growth rate of N in T is only to simplify the exposition of the remainder term in the Bahadur representation (3.10). The asymptotic distribution of $\widetilde{\beta}_g(\tau_k)$ holds even without this restriction.

With Corollary 3 and Lemma 1, we can further obtain the limiting distribution of our quantile slope estimates stated in the following theorem.

Theorem 3. *Suppose Assumptions 1–4 hold. If* $T(\log N)^2/N \to 0$ *and* N *grows at most polynomially in* T*, we have*

$$\sqrt{NT}(\widehat{\beta}_g(\tau_k) - \beta_g^0(\tau_k)) \xrightarrow{D} \mathbb{N}(\mathbf{0}, \tau_k(1-\tau_k)\Gamma_g^{-1}V_g\Gamma_g^{-1}).$$

The asymptotic convariance matrix of $\widehat{\beta}_g(\tau_k)$, $\tau_k(1-\tau_k)\Gamma_g^{-1}V_g\Gamma_g^{-1}$, depends on the conditional

density of $\{\varepsilon_{it}(\tau_k)\}$. To compute this covariance matrix, one can consider estimating Γ_g and V_g using a kernel approach. Specifically, let $\widetilde{K}(\cdot)$ denote a kernel function, such as the normal or Epanechnikov kernel, $b = b_{N,T} > 0$ denotes the bandwidth, satisfying $b \to 0$ as N and $T \to \infty$, and define the scaled kernel as $\widetilde{K}_b(z) := b^{-1}\widetilde{K}(z/b)$. Under Assumptions 1(*i*), 4(*i*) and 4(*ii*), for unit i such that $\widehat{h}_i = h$ and $\widehat{g}_i = g$, we can estimate the density function of $\varepsilon_{it}(\tau_k)$ at 0, $f_{i,\tau_k}(0)$, by

$$\widehat{f}_{hg,\tau_k} = \frac{1}{\widehat{N}_{h,g}T} \sum_{i:\widehat{h}_i=h,\widehat{g}_i=g} \sum_{t=1}^{T} \widetilde{K}_b(\widehat{\epsilon}_{it}(\tau_k)),$$

where $\widehat{N}_{h,g} = \sum_{i=1}^{N} I\{\widehat{h}_i = h, \widehat{g}_i = g\}$ is the number of units in the h-th and g-th group, and $\widehat{\epsilon}_{it}(\tau_k) = y_{it} - \widehat{\alpha}_{\widehat{h}_i}(\tau_k) - \widehat{\lambda}_t(\tau_k) - x_{it}'\widehat{\beta}_{\widehat{g}_i}(\tau_k)$ is the estimate of $\epsilon_{it}(\tau_k)$. Then we can estimate Γ_g and V_g by

$$\widehat{\Gamma}_g = \frac{1}{NT} \sum_{h\in\{1,\ldots,H\}} \sum_{i:\widehat{h}_i=h,\widehat{g}_i=g} \sum_{t=1}^{T} \widetilde{K}_b(\widehat{\epsilon}_{it}(\tau_k)) x_{it}(x_{it} - \widehat{\iota}_{h,g})',$$

$$\widehat{V}_g = \frac{1}{NT} \sum_{h\in\{1,\ldots,H\}} \sum_{i:\widehat{h}_i=h,\widehat{g}_i=g} \sum_{t=1}^{T} (x_{it} - \widehat{\iota}_{h,g})(x_{it} - \widehat{\iota}_{h,g})',$$

where $\widehat{\iota}_{h,g} = 1/(\widehat{N}_{h,g}T\widehat{f}_{hg,\tau_k}) \sum_{i:\widehat{h}_i=h,\widehat{g}_i=g}^{N} \sum_{t=1}^{T} \widetilde{K}_b(\widehat{\epsilon}_{it}(\tau_k)) x_{it}$. With these estimators, the kernel estimator of the covariance matrix can be obtained as $\tau_k(1-\tau_k)\widehat{\Gamma}_g^{-1}\widehat{V}_g\widehat{\Gamma}_g^{-1}$, whose consistency follows from the consistency of the slope and membership estimators provided in Corollaries 1 and 2.

Theorem 3 relies on large N and T, such that the estimation error of group memberships can be ignored in β-inference owe to the superconsistency of membership estimates (see Theorem 2 and Corollary 3). If one wishes to account for the misclassification error in some applications with short time periods, a practical solution is to employ the bootstrap method, which resamples unit-specific blocks from the original data and compute the variance using these resampled data (see, e.g., Bonhomme and Manresa, 2015b). Numerical performance of bootstrap inference in standard quantile panel regressions has been documented in Galvao and Montes-Rojas (2015), and its theoretical justifications are recently studied in Galvao et al. (2021). It deserves future studies to investigate the theoretical properties of bootstrapping in quantile panel regressions with latent group structures.

Remark 4. *In practice, the estimated quantile regression curves may cross, violating the logical monotonicity requirement. To address this problem, one can add an additional step to re-estimate the regression quantiles following the idea of Bondell et al. (2010). Specifically, with estimated group membership* $\{\widehat{h}_i, \widehat{g}_i\}$ *obtained from Algorithm 1, we can re-estimate* $\alpha_{\widehat{h}_i}(\tau_k)$, $\lambda_t(\tau_k)$ *and* $\beta_{\widehat{g}_i}(\tau_k)$ *by minimizing the following constrained composite check function,*

$$\min_{\boldsymbol{\theta}(\boldsymbol{\tau})\in\Theta} \frac{1}{NT} \sum_{i=1}^{N} \sum_{t=1}^{T} \sum_{k=1}^{K} \rho_{\tau_k}\left(y_{it} - \alpha_{\widehat{h}_i}(\tau_k) - \lambda_t(\tau_k) - x_{it}'\beta_{\widehat{g}_i}(\tau_k)\right),$$

$$s.t. \quad \alpha_{\widehat{h}_i}(\tau_k) + \lambda_t(\tau_k) + x_{it}'\beta_{\widehat{g}_i}(\tau_k) \geq \alpha_{\widehat{h}_i}(\tau_{k-1}) + \lambda_t(\tau_{k-1}) + x_{it}'\beta_{\widehat{g}_i}(\tau_{k-1}) \quad \textit{for } k = 2, \ldots, K.$$

According to Bondell et al. (2010) and Corollary 3, the resulting constrained coefficient estimates are asymptotically equivalent to the unconstrained estimates with known group memberships.

4 Determining the number of groups

Thus far, we assumed that the numbers of groups G and H are known. However, these numbers are often unknown in applications and must be estimated. A popular approach is to minimize some information criterion (IC) (see, e.g., Bonhomme and Manresa, 2015a; Su et al., 2016; Gu and Volgushev, 2019). Thus we consider determining the numbers of groups for the two group structures (G, H) using the following criterion:

$$\mathrm{IC}(G,H) = \frac{1}{NT}\sum_{k=1}^{K}\sum_{i=1}^{N}\sum_{t=1}^{T}\rho_{\tau_k}\left(y_{it} - \widehat{\alpha}_{\widehat{h}_i}^{(G,H)}(\tau_k) - \widehat{\lambda}_t^{(G,H)}(\tau_k) - x_{it}'\widehat{\beta}_{\widehat{g}_i}^{(G,H)}(\tau_k)\right) + \kappa K np\,(G,H)\,, \quad (4.1)$$

where the superscript (G, H) refers to the estimators obtained under G and H groups for the two group structures, $np(G, H)$ is the total number of parameters which sums the number of group membership parameters and quantile-specific parameters for all $\tau_k, k = 1, \ldots, K$, and κ is the tuning parameter. We decide the numbers of groups by minimizing the IC with respect to (G, H) that ranges from 1 to some pre-specified maximum finite numbers of groups $(G_{\max}, H_{\max})$, respectively, namely,

$$(\widehat{G}, \widehat{H}) = \arg \min_{\substack{1\le G\le G_{\max},\\ 1\le H\le H_{\max}}} \mathrm{IC}(G,H). \quad (4.2)$$

To show the consistency of $(\widehat{G}, \widehat{H})$, we denote

$$\widehat{\sigma}(\gamma_g, \gamma_h) := \frac{1}{NT}\sum_{k=1}^{K}\sum_{i=1}^{N}\sum_{t=1}^{T}\rho_{\tau_k}\left(y_{it} - \widehat{\alpha}_{h_i}^{(G,H)}(\tau_k) - \widehat{\lambda}_t^{(G,H)}(\tau_k) - x_{it}'\widehat{\beta}_{g_i}^{(G,H)}(\tau_k)\right),$$

where the fixed effects and slope coefficients are estimated under some G- and H-partition (γ_g, γ_h). Also define $\sigma_0 := \mathrm{plim}_{N,T\to\infty}\frac{1}{NT}\sum_{k=1}^{K}\sum_{i=1}^{N}\sum_{t=1}^{T}\rho_{\tau_k}\big(y_{it} - \alpha_{h_i^0}^0(\tau_k) - \lambda_t^0(\tau_k) - x_{it}'\beta_{g_i^0}^0(\tau_k)\big)$, where the superscript 0 represents the true value, and plim denotes the limit of convergence in probability. Denote (G_0, H_0) as the true number of groups.

Assumption 5.

(*i*) $\mathrm{plim}_{N,T\to\infty}\min_{1\le G<G_0}\inf_{\gamma_g\in\Gamma_G,\gamma_h\in\Gamma_H}\widehat{\sigma}(\gamma_g,\gamma_h) > \sigma_0$ for $H \le H_{\max}$;
$\mathrm{plim}_{N,T\to\infty}\min_{1\le H<H_0}\inf_{\gamma_g\in\Gamma_G,\gamma_h\in\Gamma_H}\widehat{\sigma}(\gamma_g,\gamma_h) > \sigma_0$ for $G \le G_{\max}$.

(*ii*) $\lim_{N,T\to\infty}\kappa = 0$ and $\lim_{N,T\to\infty}\sqrt{N}\exp(T\epsilon)\cdot\kappa \in (0,\infty]$ for all $\epsilon > 0$.

Assumption 5(*i*) requires that the value of the composite-quantile objective function of any underfitted model is larger than that of the true model, and this condition in conjunction with the first part of Assumption 5(*ii*) prevents underestimation of the number of groups. The second part of Assumption 5(*ii*) helps to rule out the possibility of overestimating the number of groups.

Theorem 4. *Under the conditions of Corollary 2 and Assumption 5, we have* $\mathsf{P}\{(\widehat{G},\widehat{H})=(G_0,H_0)\}\to 1$ *as* N *and* $T\to\infty$.

While the proposed IC works well when the group structures are common across the quantiles as we have assumed, a word of caution here is that if the clustering signals are distinct across quantiles, for example, strong group separation at some quantiles but very weak separation at the others, then those quantiles with weak clustering signals may "contaminate" the behavior of the IC which is based on the composite-quantile objective function. Such contamination may result in under-specification of G and H in finite samples, which may further result in inconsistent slope estimates. An alternative procedure is to first determine the optimal number of groups at each specific quantile separately based on the quantile-specific IC (rather than the composite IC), and then choose the maximum number over all considered quantiles. This procedure avoids contamination by quantiles with weak clustering signals, but is more sensitive and may favor a larger numbers of groups due to the estimation noise, especially at the tail quantiles.

5 Monte Carlo simulation

In this section, we evaluate the finite-sample performance of the proposed method. Specifically, we examine if our method can accurately classify units and effectively recover the quantile-specific slope coefficients within each group. We compare our approach with mean-based multi-dimensional clustering and composite-quantile one-dimensional clustering to shed light on the importance of considering the entire distribution and multi-dimensional structures when clustering.

5.1 Data generation process

We consider four data generation processes (DGPs) that differ in the distribution of errors and the multi-dimensional group structures.

DGP.1: We focus on the location-scale shift model:

$$y_{it}=\alpha_{h_i}+\lambda_t+\beta_{g_i}x_{it}+(1+\psi x_{it})\epsilon_{it},\quad h_i=1,\ldots,H_0;\ g_i=1,\ldots,G_0, \tag{5.1}$$

where we set $\psi=0.5$ and λ_t follows a standard uniform distribution, that is, $U(0,1)$. Following Kato et al. (2012), we generate $x_{it}=0.3(\alpha_{h_i}+\lambda_t)+z_{it}$, where z_{it} is independently and identically generated by χ^2_5. The error term ϵ_{it} is i.i.d. and follows a standard normal distribution. There are two groups for slope coefficients ($G_0=2$) but four groups for cross-section fixed effects ($H_0=4$). Each g-group contains Ng_1 and Ng_2 individual units, respectively, and $Ng_1+Ng_2=N$. We fix the ratio among these two groups such that $Ng_1:Ng_2=0.5:0.5$. In this DGP, we consider that the group structure of fixed effects nests that of slopes, namely $h_i^0=h_j^0$ implying $g_i^0=g_j^0$, and we fix the ratio of the number of units in the four h-groups as $Nh_1:Nh_2:Nh_3:Nh_4=$

$0.25 : 0.25 : 0.25 : 0.25$. In other words, the h-group structure further segments each g-group into two equally-sized groups. The group-specific intercept and slope coefficient are set as

$$(\alpha_1, \alpha_2, \alpha_3, \alpha_4)' = (-5, -2.5, 2.5, 5)', \quad (\beta_1, \beta_2)' = (-0.75, 0.75)'.$$

In this case, groups are separated in their means, while the shape of their distributions is common (see Figure 2(a) for the density function of $\beta_{g_i} + \psi\epsilon_{it}$).

DGP.2: In practice, the groups may differ not only in their means but also in their shapes of distribution. To mimic this situation, we consider the case with heterogeneous intercepts and slopes, and the distribution of the error term is also allowed to vary across the groups. We generate two groups of errors following the same group structure of slope coefficients. The first group of errors follows a standard normal distribution, while the second group follows a Weibull distribution. By subtracting the *theoretical* mean, the errors of the two groups follow heterogeneous distributions with mean zero but distinct tail behavior. In particular, we generate

$$\epsilon_{it} \sim \begin{cases} \text{i.i.d. } N(0,1) & \text{if } g_i = 1, \\ \text{i.i.d. Weibull}(sh, sc) - E[\text{Weibull}(sh, sc)] & \text{if } g_i = 2, \end{cases} \tag{5.2}$$

where $sh = 3$ and $sc = 1$ are the shape and scale parameters of the Weibull distributions, respectively. See Figure 2(b) for the density function of slope coefficients. Other settings remain the same as in DGP.1.

DGP.3: This case allows the two group structures γ_h and γ_g to be non-nested. Particularly, we generate the four h-groups by assigning the first quarter of units to Group 1, the second quarter to Group 2, the third quarter to Group 3, and the fourth quarter to Group 4. The g-group structure assigns the first $3/8$ of units to Group 1 and the remaining to Group 2. This way of generating memberships leads to two non-nested group structures with a smaller fraction of overlap than those in DGP.1. Other settings remain the same as DGP.1.

DGP.4: Same as DGP.3 except that the distributions of errors are heterogeneous as in DGP.2.

For each DGP, we consider two cross-sectional sample sizes, $N = (80, 160)$, and two lengths of time series, $T = (20, 40)$, leading to four combinations of cross-sectional and time series dimensions. The number of replications is set to 1000.

5.2 Implementation and evaluation

We apply Algorithm 1 to obtain two-dimensional clustering using composite quantiles $\tau \in \{0.1, 0.2, \ldots, 0.9\}$, and refer to it as 2D-CQ. We compare it with mean-based two-dimensional clustering and single-dimensional composite-quantile clustering estimators.

The mean-based two-dimensional clustering is an extension of the GFE estimator (Bonhomme and Manresa, 2015a) to two-dimensional group structures, or can be viewed as a least squares version of

Figure 2: Density of $\beta_{g_i} + \psi\epsilon_{it}$ for the two groups in the simulation

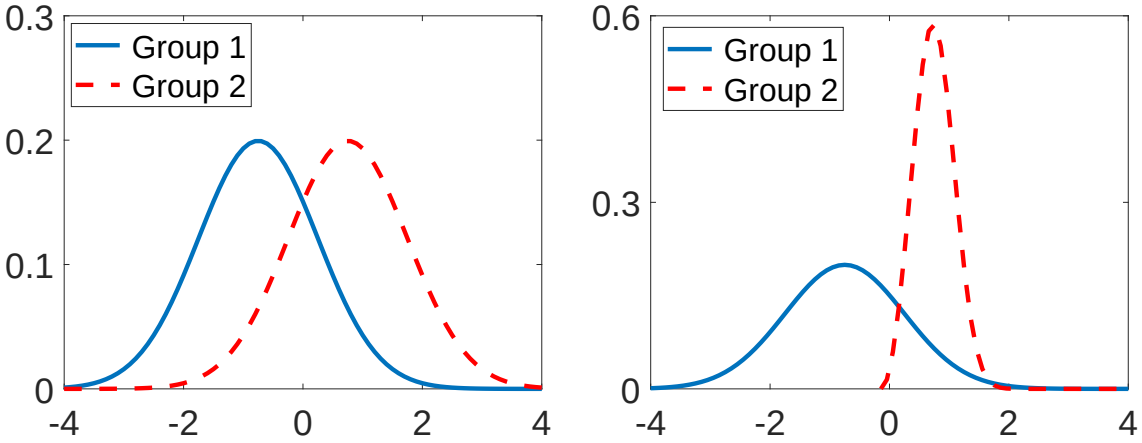

(a) DGP.1 and DGP.3 (b) DGP.2 and DGP.4

Cheng et al. (2019)'s multi-dimensional clustering. It estimates the two latent group structures, fixed effects, and slope parameters by minimizing the following objective function:

$$\arg\min_{\gamma_h,\gamma_g,\boldsymbol{\alpha},\boldsymbol{\beta},\boldsymbol{\lambda}} \frac{1}{NT}\sum_{i=1}^{N}\sum_{t=1}^{T}\left(y_{it}-\alpha_{h_i}-\lambda_t-x_{it}'\beta_{g_i}\right)^2.$$

The above optimization problem can be solved by applying the similar iterative algorithm as Algorithm 1 but replacing the quantile check function with least squares, and we refer to the resulting estimates as 2D-GFE.

The single-dimensional composite-quantile clustering (1D-CQ) approach requires a common group structure for both cross-section fixed effects and slopes, and it estimates the parameters by solving the following optimization problem:

$$\arg\min_{\gamma,\boldsymbol{\alpha}(\boldsymbol{\tau}),\boldsymbol{\beta}(\boldsymbol{\tau}),\boldsymbol{\lambda}(\boldsymbol{\tau})} \frac{1}{NT}\sum_{i=1}^{N}\sum_{t=1}^{T}\sum_{k=1}^{K}\rho_{\tau_k}\left(y_{it}-\alpha_{g_i}(\tau_k)-\lambda_t(\tau_k)-x_{it}'\beta_{g_i}(\tau_k)\right),\ g_i=1,\ldots,G_{1D},$$

where G_{1D} is the number of groups that guarantees homogeneity in a group for single-dimensional clustering. Since 1D-CQ requires more strict requirements of homogeneity within a group, it works with the same or larger number of groups than the multi-dimensional clustering, namely $G_{1D} = 4$ in DGPs 1 and 2 where the cross-section group structure nests that of the slopes, and $G_{1D} = 5$ in DGPs 3 and 4 where the two group structures are not nested. We use the same quantile range $\tau \in \{0.1, 0.2, \ldots, 0.9\}$ as in 2D-CQ. This approach resembles the multiple-quantile clustering with a single-dimensional group structure by Zhang et al. (2019a).

We evaluate the performance of the proposed method based on clustering, the coefficient estimates across quantiles, and selecting the right number of groups. First, we measure clustering accuracy given the correct number of groups by taking the average of the misclustering frequency across replications.

Let $I(\cdot)$ be the indicator function. The overall MF is computed as

$$\text{MF}_{\text{overall}} = 1 - \frac{1}{N}\sum_{i=1}^{N} I(\widehat{g}_i = g_i^0, \widehat{h}_i = h_i^0).$$

We also report the MF for cross-section effects (MF_H) and slope coefficients (MF_G) separately, i.e.,

$$\text{MF}_H = 1 - \frac{1}{N}\sum_{i=1}^{N} I(\widehat{h}_i = h_i^0), \quad \text{and} \quad \text{MF}_G = 1 - \frac{1}{N}\sum_{i=1}^{N} I(\widehat{g}_i = g_i^0).$$

Second, we evaluate the accuracy of the slope coefficient estimates at each quantile, also given the correct number of groups, based on their bias and root mean squared error (RMSE) computed, respectively, as

$$\text{Bias}(\widehat{\beta}(\tau)) = \frac{1}{G}\sum_{g=1}^{G}\left[\widehat{\beta}_g(\tau) - \beta_g^0(\tau)\right], \quad \text{and} \quad \text{RMSE}(\widehat{\beta}(\tau)) = \sqrt{\frac{1}{G}\sum_{g=1}^{G}\left[\widehat{\beta}_g(\tau) - \beta_g^0(\tau)\right]^2},$$

where $G = G_0$ for 2D-CQ and $G = G_{1D}$ for 1D-CQ. Finally, we examine how the IC-based procedure performs in determining the number of groups. In practice, to compute the IC, we find that $\kappa = 1.5\log(NT)/\sqrt{NT}$ works fairly well based on a large number of experiments with many alternatives, and we employ this penalty in all simulations and the application. Our penalty term in (4.1) is comparable to the Bayesian Information Criterion (BIC) proposed by Bonhomme and Manresa (2015b) and Cheng et al. (2019). Performance is evaluated by the empirical probability of selecting a specific number.[9]

5.3 Results

Clustering accuracy

First, we examine clustering performance. Table 1 presents the overall MF and separate MFs for the two-dimensional groups. In general, we find that 2D-CQ produces a lower MF than 2D-GFE and 1D-CQ in all the cases and increasing the time dimension significantly reduces the MF for all the methods. Specifically, in DGPs 1 and 2, where the two-dimensional group structures are nested, 2D-CQ misclassifies less than 6% units when $N = 80$ and $T = 20$. Further examination reveals that misclustering only occurs for cross-section effects but not for slope coefficients, because cross-section effects are more difficult to estimate than slope parameters due to fewer units in h-groups ($H > G$) and less variation of the unit dummy than the explanatory variable. As T increases to 40, the $\text{MF}_{\text{overall}}$ of 2D-CQ reduces to around 1%. 2D-GFE can also accurately capture slope heterogeneity ($\text{MF}_G = 0$) in these two DGPs, but produces higher MF_H for cross-section effects than 2D-CQ. This result suggests that employing information at multiple quantiles improves clustering when a grouped

[9] We also consider the alternative two-step procedure of first determining the numbers for each quantile and then choosing the maximum ones. The results are qualitatively similar and thus omitted here.

pattern of heterogeneity is common across different quantiles of the distribution. The MF of 1D-CQ is higher than the $\text{MF}_{\text{overall}}$ of 2D-CQ, but generally lower than that of 2D-GFE. This result, on the one hand, highlights the importance of accounting multi-dimensional group structures; but on the other hand, demonstrates the benefits of using composite quantiles when clustering.

In DGP.3 where the two-dimensional group structures are not nested, 2D-CQ continues to perform well and its overall misclustering frequency is less than 9% when $T = 20$ and further reduced to less than 5% when $T = 40$. While 1D-CQ produces a similar MF when $T = 20$, the convergence as T increases is much slower than 2D-CQ. This is because it imposes more groups and thus leaves less units in some groups, further causing group-specific parameters and memberships to be estimated less accurately. A similar comparison is observed in DGP.4.

Table 1: Misclustering frequencies

		$N = 80$		$N = 160$		$N = 80$		$N = 160$	
		$T = 20$	$T = 40$	$T = 20$	$T = 40$	$T = 20$	$T = 40$	$T = 20$	$T = 40$
		DGP.1				DGP.2			
2D-CQ	$\text{MF}_{\text{overall}}$	0.055	0.010	0.045	0.012	0.039	0.016	0.039	0.008
	MF_H	0.055	0.010	0.045	0.012	0.039	0.016	0.039	0.008
	MF_G	0.000	0.000	0.000	0.000	0.000	0.000	0.000	0.000
2D-GFE	$\text{MF}_{\text{overall}}$	0.093	0.025	0.081	0.024	0.051	0.022	0.061	0.020
	MF_H	0.093	0.025	0.081	0.024	0.051	0.022	0.061	0.020
	MF_G	0.001	0.000	0.001	0.000	0.000	0.000	0.000	0.000
1D-CQ		0.078	0.017	0.068	0.018	0.057	0.017	0.054	0.010
		DGP.3				DGP.4			
2D-CQ	$\text{MF}_{\text{overall}}$	0.082	0.039	0.070	0.045	0.015	0.010	0.009	0.008
	MF_H	0.081	0.039	0.070	0.045	0.015	0.010	0.009	0.008
	MF_G	0.004	0.003	0.004	0.003	0.000	0.000	0.001	0.000
2D-GFE	$\text{MF}_{\text{overall}}$	0.103	0.046	0.100	0.047	0.023	0.013	0.031	0.016
	MF_H	0.103	0.046	0.100	0.047	0.023	0.013	0.031	0.016
	MF_G	0.016	0.006	0.022	0.024	0.007	0.009	0.012	0.003
1D-CQ		0.085	0.075	0.069	0.061	0.019	0.030	0.018	0.031

Notes: 2D-CQ is the proposed composite-quantile two-dimensional clustering with $\tau = \{0.1, 0.2, \ldots, 0.9\}$; 2D-GFE is mean-based two-dimensional clustering; 1D-CQ is composite-quantile single-dimensional clustering with $\tau = \{0.1, 0.2, \ldots, 0.9\}$ and the number of groups $G_{1D} = 4$ in DGPs 1 and 2, and $G_{1D} = 5$ in DGPs 3 and 4. $\text{MF}_{\text{overall}}$ is the overall misclustering frequency, $1 - 1/N \sum_{i=1}^{N} I(\hat{g}_i = g_i^0, \hat{h}_i = h_i^0)$; MF_H is the frequency for cross-section fixed effects, $1 - 1/N \sum_{i=1}^{N} I(\hat{h}_i = h_i^0)$; MF_G is the frequency for slope coefficients, $1 - 1/N \sum_{i=1}^{N} I(\hat{g}_i = g_i^0)$.

Accuracy of the regression quantile estimates

Next, we examine the accuracy of slope coefficient estimates, and report the bias and RMSE of the three estimators in Table 2. Like the standard quantile regression, the 2D-CQ coefficient estimates are

more accurate at the central quantiles than at the tails. Comparing the 2D-CQ coefficient estimates at the median with those of 2D-GFE, the former generally have a lower bias and RMSE due to more accurate clustering by using composite quantiles, especially in DGP.4. The superiority of 2D-CQ is more obvious compared with 1D-CQ, with the improvement of RMSEs as high as more than 50% in many cases. The better performance of 2D-CQ coefficient estimates is attributed to separate estimation of the two group structures and thus more accurate clustering for slope coefficients.

Determining the number of groups

Finally, we examine how the IC-based procedure performs in determining the number of groups. We use the IC defined in (4.1) to select the number of groups at composite quantiles $\tau_k = 0.1, 0.2, \ldots, 0.9$. Table 3 provides the empirical probability of selecting specific number of groups, ranging G and H from 1 to 6. Recall that the true number of groups is $H_0 = 4$ and $G_0 = 2$. The results show that our method can effectively detect the precise number of groups in most cases and the frequency of selecting the correct number generally increases with the time dimension.

6 Managerial incentives and risk taking

In this section, we study the economic importance of accounting for distributional heterogeneity by revisiting the relationship between managerial incentives and risk-taking behavior. Coles et al. (2006) examined the impact of managerial incentives on R&D expenditures scaled by total assets (RD). They employed linear panel models with additive industry-time fixed effects and homogeneous coefficients across firms, and found that higher sensitivity of CEO wealth to stock return volatility (vega) leads to riskier policy choices, such as higher investment in R&D. In fact, the impact of managerial incentives on R&D expenditure may significantly vary across different levels of expenditure, given the highly skewed distribution of the expenditure. This effect is also likely to differ dramatically across firms due to a heterogeneous corporate strategy, risk attitude, and managerial characteristics. Moreover, the unobserved cross-sectional heterogeneity may not be at the industry level but more complicatedly depend on unobserved firm and managerial characteristics. Therefore, industry fixed effects or industry-based grouping may not fully capture the unobserved cross-sectional heterogeneity. To capture the heterogeneous distributional effects and allow for more flexible unobserved cross-sectional heterogeneity, we examine the same empirical question as Coles et al. (2006) using the MuGS-QR model as:

$$Q_\tau(\mathrm{RD}_{it}|x_{it}) = \alpha_{h_i}(\tau) + \lambda_t(\tau) + \mathrm{vega}_{it-1}\beta_{1g_i}(\tau) + \mathrm{delta}_{it-1}\beta_{2g_i}(\tau) + x_{it}'\beta_{cg_i}(\tau), \tag{6.1}$$

where lagged vega (lvega, the dollar change in the value of the CEO's wealth for a 1% change in standard deviation of returns) and lagged delta (ldelta, the dollar change in the value of the CEO's wealth for a 1% change in stock price) both measure managerial incentives, and x_{it} contains salient controls as in Coles et al. (2006), namely cash compensation (comp), log of sales (lsale), market-to-

Table 2: Accuracy of coefficient estimates

			$N = 80$				$N = 160$			
			$T = 20$		$T = 40$		$T = 20$		$T = 40$	
		τ	Bias	RMSE	Bias	RMSE	Bias	RMSE	Bias	RMSE
DGP.1	2D-CQ	0.3	0.023	0.071	0.015	0.047	0.008	0.043	0.005	0.025
		0.5	0.005	0.061	0.006	0.042	0.001	0.041	0.001	0.030
		0.7	−0.002	0.061	0.000	0.039	−0.008	0.042	−0.002	0.035
	2D-GFE		0.013	0.073	0.010	0.040	0.002	0.044	0.007	0.030
	1D-CQ	0.3	0.039	0.147	0.013	0.071	0.015	0.096	−0.014	0.080
		0.5	0.015	0.136	0.008	0.064	0.000	0.098	−0.018	0.085
		0.7	−0.002	0.143	0.004	0.070	−0.010	0.096	−0.020	0.089
DGP.2	2D-CQ	0.3	0.015	0.164	0.012	0.167	0.015	0.162	−0.002	0.174
		0.5	0.009	0.045	0.009	0.034	0.008	0.031	−0.002	0.018
		0.7	0.005	0.187	0.003	0.182	−0.003	0.179	−0.001	0.179
	2D-GFE		0.004	0.041	0.007	0.038	0.005	0.034	−0.004	0.022
	1D-CQ	0.3	0.035	0.191	0.010	0.176	0.023	0.168	0.000	0.176
		0.5	0.015	0.105	0.008	0.048	0.011	0.080	−0.003	0.035
		0.7	0.012	0.214	0.004	0.189	−0.003	0.193	0.000	0.183
DGP.3	2D-CQ	0.3	0.039	0.076	0.037	0.056	0.031	0.062	0.038	0.050
		0.5	0.020	0.064	0.024	0.049	0.010	0.046	0.020	0.037
		0.7	0.003	0.062	0.014	0.049	−0.002	0.043	0.011	0.032
	2D-GFE		0.023	0.077	0.020	0.058	0.027	0.059	0.039	0.060
	1D-CQ	0.3	0.050	0.157	0.079	0.196	0.012	0.119	0.070	0.166
		0.5	0.024	0.153	0.076	0.190	−0.001	0.114	0.066	0.163
		0.7	0.006	0.150	0.068	0.197	−0.013	0.121	0.055	0.165
DGP.4	2D-CQ	0.3	0.003	0.199	−0.013	0.196	−0.009	0.173	−0.010	0.174
		0.5	0.006	0.186	−0.006	0.167	−0.004	0.154	0.000	0.138
		0.7	0.009	0.203	−0.003	0.176	0.003	0.161	0.012	0.162
	2D-GFE		0.014	0.225	−0.003	0.219	0.014	0.209	0.004	0.163
	1D-CQ	0.3	0.028	0.324	0.054	0.392	0.028	0.320	0.037	0.339
		0.5	0.019	0.306	0.046	0.378	0.022	0.302	0.038	0.324
		0.7	0.012	0.295	0.038	0.368	0.016	0.296	0.033	0.309

Notes: 2D-CQ is the proposed two-dimensional composite-quantile clustering with $\tau = \{0.1, 0.2, \ldots, 0.9\}$; 2D-GFE is mean-based two-dimensional clustering; 1D-CQ is single-dimensional composite-quantile clustering with $\tau = \{0.1, 0.2, \ldots, 0.9\}$ and the number of groups $G_{1D} = 4$ in DGPs 1 and 2, and $G_{1D} = 5$ in DGPs 3 and 4.

Table 3: Group number selection frequency using IC when $H_0 = 4$ and $G_0 = 2$

N	T		1	2	3	4	5	6	1	2	3	4	5	6
			DGP.1						DGP.2					
80	20	H	0.00	0.00	0.28	**0.72**	0.00	0.00	0.00	0.00	0.21	**0.79**	0.00	0.00
		G	0.00	**0.92**	0.08	0.00	0.00	0.00	0.00	**0.83**	0.17	0.00	0.00	0.00
80	40	H	0.00	0.00	0.22	**0.78**	0.00	0.00	0.00	0.00	0.06	**0.94**	0.00	0.00
		G	0.00	**0.94**	0.06	0.00	0.00	0.00	0.00	**0.90**	0.10	0.00	0.00	0.00
160	20	H	0.00	0.00	0.01	**0.98**	0.01	0.00	0.00	0.00	0.11	**0.85**	0.04	0.00
		G	0.00	**0.87**	0.13	0.00	0.00	0.00	0.00	**0.71**	0.29	0.00	0.00	0.00
160	40	H	0.00	0.00	0.00	**1.00**	0.00	0.00	0.00	0.01	0.04	**0.91**	0.04	0.00
		G	0.00	**1.00**	0.00	0.00	0.00	0.00	0.00	**0.77**	0.23	0.00	0.00	0.00
			DGP.3						DGP.4					
80	20	H	0.00	0.14	0.14	**0.72**	0.00	0.00	0.00	0.00	0.00	**0.87**	0.13	0.00
		G	0.00	**0.73**	0.27	0.00	0.00	0.00	0.00	**0.75**	0.24	0.01	0.00	0.00
80	40	H	0.00	0.01	0.16	**0.81**	0.01	0.00	0.00	0.00	0.00	**0.98**	0.02	0.00
		G	0.00	**0.61**	0.36	0.03	0.00	0.00	0.00	**0.80**	0.10	0.10	0.00	0.00
160	20	H	0.00	0.00	0.10	**0.81**	0.09	0.00	0.00	0.00	0.00	**1.00**	0.00	0.00
		G	0.00	**0.63**	0.34	0.03	0.00	0.00	0.00	**0.62**	0.27	0.11	0.00	0.00
160	40	H	0.00	0.00	0.03	**0.90**	0.07	0.00	0.00	0.00	0.00	**1.00**	0.00	0.00
		G	0.00	**0.67**	0.30	0.03	0.00	0.00	0.00	**0.68**	0.23	0.09	0.00	0.00

book ratio (mb), and surplus cash (cash); See Coles et al. (2006) for detailed definition of the control variables. Instead of imposing a specific pattern of heterogeneity, for instance, industry grouping, we allow cross-section fixed effects and slope coefficients to vary flexibly across groups, and the group structures of the fixed effects and slopes can be arbitrarily different. We estimate the two latent group structures from the data. Our specification of group-time fixed effects facilitates comparison with the industry-time fixed effects model in Coles et al. (2006), and is justified by ample empirical evidence that firm unobserved heterogeneity has a grouped pattern, such that a group of firms share similar financial constraints, management practices, corporate governance, and firm's supply chain network (see, e.g., Mitton, 2002; Duchin et al., 2010, among others).

Our sample is constructed from 1997 to 2010 and contains 188 firms, which is the maximum possible number if we wish to obtain a balanced panel. Data on CEO compensation are from the Standard & Poor's Execucomp database, firm-specific information is obtained from Compustat, and stock return information from the Center for Research in Security Prices (CRSP). We estimate model (6.1) with $G = 3$ and $H = 5$, the numbers suggested by our IC, and compare the estimates with those from the linear panel models with industry-time fixed effects as in Coles et al. (2006).

Table 4 presents the coefficient estimates of different methods. All coefficient estimates and their standard deviations are multiplied by 100. The first column provides the industry-time fixed effects estimates (using least squares), and we largely replicate the results of Coles et al. (2006) by obtaining strong and positive effect of vega but insignificant delta. The estimates of other controls are also of the same sign and significance as in Coles et al. (2006). The second column presents the MuGS-QR estimates with $G = H = 1$ (or equivalently, homogeneous panel quantile regression with time fixed effects) at $\tau = 0.5$, and they resemble the estimates in the first column. The remaining columns of Table 4 present the MuGS-QR estimates with $G = 3$ and $H = 5$. The estimates of Group 1 are all close to zero because this group contains firms with little or no R&D expenditure. Detailed discussions on the group structure follows. In the other two groups, we find that the impact of managerial incentives varies significantly across groups and across quantiles. Particularly, the impact of the lagged vega is positive at the central or low quantiles but negative at the upper quantiles for both groups, and it is much stronger and more significant in Group 3 than in Group 2. Further examination reveals that the firms in Group 3 are characterized by higher R&D expenditure and other firm variables than those in Group 2 (see Table 5). This result suggests that for large firms with substantial expenditure on R&D, a higher level of vega, associated with higher option-based compensation and thus more convex payoffs, helps to reduce risk aversion and encourages managers to invest more on R&D. However, for relatively smaller firms and those that do not need much R&D expenditure, the association between managerial incentives and R&D expenditure is less obvious. As for the effect of lagged delta, the difference between the two groups is even more profound: positively significant in Group 2 but negatively significant in Group 3. The sensitivity of delta (which measures CEO wealth to stock price) is consistent with the theory that it has a two-fold impact on risk-taking (Coles et al., 2006). On the one hand, managers are undiversified with respect to firm-specific wealth following an increase in delta, and thus exposed to more risk. This may further result in more conservative policies and forgoing of risky projects even

Table 4: Managerial incentives and risk-taking behavior (×100)

	Industry-time FE	MuGS-QR $G=H=1$	MuGS-QR $G=3, H=5$								
τ		0.5	0.1	0.2	0.3	0.4	0.5	0.6	0.7	0.8	0.9
			Group 1								
lvega	1.749	2.860	0.000	0.000	0.000	0.000	0.000	0.000	0.000	0.000	0.000
	(0.413)	(0.470)	(0.223)	(0.000)	(0.221)	(0.250)	(0.268)	(0.245)	(0.255)	(0.240)	(0.326)
ldelta	0.015	−0.040	0.000	0.000	0.000	0.000	0.000	0.000	0.000	0.000	0.000
	(0.030)	(0.030)	(0.019)	(0.000)	(0.019)	(0.021)	(0.023)	(0.021)	(0.022)	(0.021)	(0.028)
comp	−0.218	−0.050	0.000	0.000	0.000	0.000	0.000	0.000	0.000	0.000	0.000
	(0.057)	(0.040)	(0.032)	(0.000)	(0.032)	(0.036)	(0.039)	(0.036)	(0.037)	(0.035)	(0.048)
lsale	−0.272	−0.220	0.000	0.000	0.000	0.000	0.000	0.000	0.000	0.000	0.000
	(0.061)	(0.050)	(0.028)	(0.000)	(0.028)	(0.031)	(0.033)	(0.030)	(0.032)	(0.030)	(0.041)
mb	−0.381	−0.340	0.000	0.000	0.000	0.000	0.000	0.000	0.000	0.000	0.000
	(0.095)	(0.090)	(0.040)	(0.000)	(0.040)	(0.045)	(0.048)	(0.044)	(0.046)	(0.043)	(0.059)
cash	27.786	25.020	0.000	0.000	0.000	0.000	0.000	0.000	0.000	0.000	0.000
	(1.772)	(1.970)	(0.840)	(0.000)	(0.835)	(0.943)	(1.011)	(0.924)	(0.962)	(0.907)	(1.232)
			Group 2								
lvega			0.556	0.386	0.239	0.081	−0.211	−0.443	−0.567	−0.797	−0.938
			(0.460)	(0.476)	(0.458)	(0.517)	(0.554)	(0.507)	(0.527)	(0.497)	(0.675)
ldelta			0.208	0.233	0.226	0.232	0.269	0.326	0.342	0.344	0.373
			(0.035)	(0.031)	(0.035)	(0.040)	(0.043)	(0.039)	(0.041)	(0.038)	(0.052)
comp			−0.055	−0.076	−0.092	−0.072	−0.087	−0.069	−0.092	−0.097	−0.203
			(0.050)	(0.048)	(0.049)	(0.056)	(0.060)	(0.055)	(0.057)	(0.054)	(0.073)
lsale			0.001	−0.005	−0.008	−0.020	−0.027	−0.038	−0.044	−0.058	−0.041
			(0.030)	(0.029)	(0.030)	(0.034)	(0.036)	(0.033)	(0.034)	(0.032)	(0.044)
mb			−0.002	0.138	0.162	0.244	0.333	0.359	0.400	0.517	0.442
			(0.070)	(0.073)	(0.070)	(0.078)	(0.084)	(0.077)	(0.080)	(0.075)	(0.102)
cash			11.095	9.759	10.890	10.568	10.083	10.677	11.092	10.845	14.728
			(1.073)	(1.064)	(1.067)	(1.205)	(1.291)	(1.181)	(1.229)	(1.158)	(1.573)
			Group 3								
lvega			0.686	1.045	1.065	1.103	1.041	0.351	0.017	−1.093	−2.353
			(0.430)	(0.478)	(0.428)	(0.483)	(0.518)	(0.473)	(0.493)	(0.464)	(0.631)
ldelta			−0.035	−0.124	−0.166	−0.187	−0.160	−0.085	−0.107	−0.038	−0.013
			(0.047)	(0.038)	(0.047)	(0.053)	(0.056)	(0.051)	(0.054)	(0.050)	(0.069)
comp			−0.710	−0.959	−1.055	−0.949	−1.080	−1.019	−1.160	−1.340	−1.661
			(0.211)	(0.218)	(0.210)	(0.238)	(0.255)	(0.233)	(0.242)	(0.228)	(0.310)
lsale			0.407	0.574	0.632	0.667	0.697	0.756	0.794	0.902	1.104
			(0.043)	(0.046)	(0.042)	(0.048)	(0.051)	(0.047)	(0.049)	(0.046)	(0.063)
mb			−0.076	0.168	0.349	0.283	0.183	0.083	0.160	0.144	−0.004
			(0.087)	(0.082)	(0.087)	(0.098)	(0.105)	(0.096)	(0.100)	(0.094)	(0.128)
cash			17.471	13.565	11.742	12.007	15.902	16.698	17.713	18.876	20.852
			(1.005)	(1.060)	(0.999)	(1.129)	(1.210)	(1.106)	(1.151)	(1.085)	(1.474)

Notes:

1. Standard deviations are given in parentheses.
2. In all regressions, the dependent variable is R&D expenditure, lvega is lagged vega, ldelta is lagged delta, comp is cash compensation, lsale is log of sales, mb is market-to-book ratio, and cash is surplus cash.
3. All coefficient estimates and their standard deviations are multiplied by 100.

though they may generate positive net present value. On the other hand, a higher delta encourages managers to work more effectively due to shared interests with shareholders, and the increase in equity-based compensation may offset the negative effect on risk-taking. The opposite effect of lagged delta in the two groups also explains the insignificant overall effect obtained from the pooled linear and panel quantile model with $G = H = 1$ (reported in the first and second column of Table 4). The impact of cash compensation, log of sales, and surplus cash also vary significantly across groups, with the effects stronger and more diversified over the quantiles in Group 3 than in Group 2.

Figure 3: Industry composition of the three groups

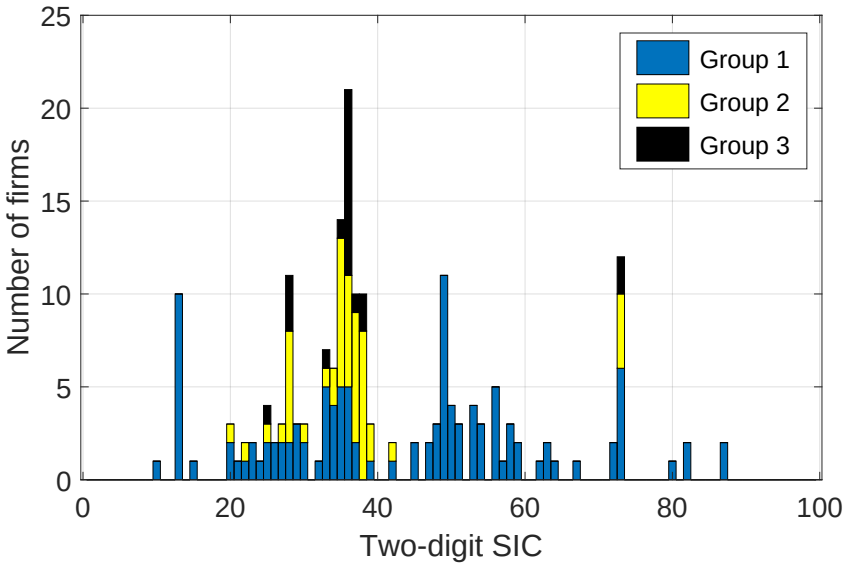

Table 5: Descriptive statistics of the three groups

	Group 1		Group 2		Group 3	
	Mean	Std.	Mean	Std.	Mean	Std.
RD	0.003	0.007	0.037	0.030	0.113	0.054
lvega	0.139	0.197	0.185	0.218	0.284	0.257
ldelta	0.813	1.940	0.912	2.231	1.115	2.239
comp	1.396	1.235	1.571	1.261	1.311	0.902
lsale	7.932	1.442	8.084	1.284	7.874	1.410
mb	1.768	1.017	2.085	1.115	2.850	1.798
cash	0.064	0.060	0.110	0.072	0.196	0.107

Notes: RD is R&D expenditure, lvega is lagged vega, ldelta is lagged delta, comp is cash compensation, lsale is log of sales, mb is market-to-book ratio, and cash is surplus cash.

To better interpret these results, we analyze the composition of the three groups. Figure 3 presents the appearance frequency of each industry (specified by the two-digit Standard Industrial Classification (SIC) code) in each group, and Table 5 provides the descriptive statistics for the firm and manager variables. Group 1 is featured by zero or very little R&D expenditure, leading to zero coefficient estimates as reported above. This group is mainly composed of firms from basic industries, such as oil

& gas extraction (SIC=13), electric, gas, & sanitary services (SIC=49), and third industries (retail, restaurants, business, etc.), which hardly require any R&D investment. Group 2 is characterized by a moderate level of R&D and mainly contains traditional manufacturing firms specializing in chemical & allied products (SIC=28), industrial machinery (SIC=35), transportation equipment (SIC=37), and instruments & related products (SIC=38). Finally, firms in Group 3 are featured by high R&D expenditure, lagged vega, market-to-book ratio, and surplus cash. The largest proportion of firms in this group is electronic & electric (SIC=36), especially in computer-related devices (e.g., INTEL Corp., Micron Technology Inc.) and semiconductor companies (e.g., Advanced Micro Devices, Analog Devices). It consists of business service companies (SIC=73), but also specializes in computer-related services, such as Electronic Arts Inc. and PTC Inc. These firms obviously require a large amount of investment in R&D and are well valued (reflected by a high market-to-book ratio). Interestingly, the value of vega in this group is also much higher than that of the other two groups, suggesting strong incentives provided to managers in these firms. This confirms the strong and positive coefficient of vega in the R&D regression at the lower and central quantiles. The negative coefficient of vega at higher quantiles is particularly due to low vega for certain firms in 1997–1998 and around 2009 when the Asian and global financial crises broke out, respectively.

Overall, we find a significant degree of heterogeneity in the relationship between managerial incentives and risk-taking behavior across groups and in the (conditional) distribution of R&D expenditure. The grouped pattern is to some extent related with but differs sufficiently from industry grouping, which is often imposed by applied finance researchers. The distributional heterogeneity and the latent group structure can be captured by our MuGS-QR model but not by the conventional two-way fixed effects approaches.

7 Conclusion and future research

This study offers a flexible yet parsimonious way of modelling the distributional heterogeneity of slope coefficients in panel data models with additive cross-section and time fixed effects. We model cross-sectional heterogeneity via a latent grouped pattern and allow the group structures of cross-section effects and slope to flexibly differ. The distributional effect within each group is captured using regression quantiles. With the underlying assumption of quantile-invariant group memberships, we propose a composite quantile approach to simultaneously estimate the two-dimensional group memberships and slope parameters. We precisely quantify the convergence rate of the MF to show that using multiple quantiles for clustering improves the accuracy of the group membership estimates over the existing methods in which clustering is only based on the mean or some single quantile.

While two-dimensional clustering offers a flexible way of capturing heterogeneity, its resulting estimates could be less efficient than one-dimensional clustering if the cross-section effects and slope coefficients share a common group structure in the DGP. This is because two-dimensional clustering estimates an unnecessarily more complex model with N extra group membership parameters. Hence, the choice between these two clustering methods should depend on the research problem and the data.

As a general practical guidance, we recommend using two-dimensional clustering when T is large, because it permits more units in a group than one-dimensional clustering and the cost of estimating two sets of membership parameters decays quickly as T increases, as shown in Theorem 2. In a different situation, when T is relatively small but there are sufficient cross-section units, we recommend using one-dimensional clustering, because the misclassification error due to small T may amplify when trying to estimate an additional set of membership parameters, while the issues of sparse interactions and small groups associated with one-dimensional clustering may become less serious when sufficient units are available.

Several issues deserve further research. First, we assume that group membership is invariant across quantiles. Zhang et al. (2019a) proposed a promising clustering consensus statistic based on perturbation techniques to verify the stability of clustering across quantiles. Alternatively, one can test the invariance of clustering across quantiles by comparing the confidence sets of group membership estimates proposed by Dzemski and Okui (2021) across quantiles to see if they are compatible. Second, the computation cost is non-trivial when the number of groups is large. Thus, it is desirable to resort to alternative algorithms that work faster and are more stable when the number of groups is large. Third, while bootstrapping works as a practical method for inference to account for the misclassification error, its behaviour and theoretical properties in quantile panel regressions with latent group structures deserves future studies. Last but not the least, we assume that cross-section fixed effects are characterized by group heterogeneity with a finite number of groups. How to estimate a panel quantile model with individual and time fixed effects remains an open but highly challenging topic.

Acknowledgements

We thank Serena Ng (Editor), the associate editor, anonymous referees, Mingli Chen, Ivan Fernandez-Val, Bo Honoré, Dennis Kristensen, Stepana Lazarova, Arthur Lewbel, Elena Manresa, Chris Muris, Ryo Okui, Liangjun Su, Yixiao Sun, Yutao Sun, Stanislav Volgushev, and Martin Weidner, the participants of seminars at the Nanyang Technological University, Erasmus University Rotterdam, Queen Mary University of London, Maastricht University, York University, and University of Sydney, 4th Conference of the International Society for Non-parametric Statistics in Salerno, and 4th Dongbei Econometrics Workshop in Dalian, CMStatistics 2018 in Pisa, RES Annual Conference 2019 in Warwick, SETA 2019 in Osaka, and ESEM 2019 in Manchester for their useful discussions and constructive comments. Leng's research is partially supported by the National Natural Science Foundation of China Grant 72001183, the Fundamental Research Fund for the Central Universities 20720201047, and the Basic Scientific Center Project 71988101 of National Science Foundation of China. Wang acknowledges the financial support of the EUR Fellowship.

References

T. Ando and J. Bai. Panel data models with grouped factor structure under unknown group membership. *Journal of Applied Econometrics*, 31:163–191, 2016.

H. D. Bondell, B. J. Reich, and H. Wang. Noncrossing quantile regression curve estimation. *Biometrika*, 97:825–838, 2010.

S. Bonhomme and E. Manresa. Grouped patterns of heterogeneity in panel data. *Econometrica*, 83: 1147–1184, 2015a.

S. Bonhomme and E. Manresa. Supplement to 'grouped patterns of heterogeneity in panel data'. *Econometrica Supplemental Material*, 83:1147–1184, 2015b.

S. Bonhomme, T. Lamadon, and E. Manresa. Discretizing unobserved heterogeneity. Working paper, 2017.

S. Bonhomme, T. Lamadon, and E. Manresa. A distributional framework for matched employer employee data. *Econometrica*, 87:699–739, 2019.

R. C. Bradley. On the spectral density and asymptotic normality of weakly dependent random fields. *Journal of Theoretical Probability*, 5:355–373, 1992.

J. E. Brand and Y. Xie. Who benefits most from college? Evidence for negative selection in heterogeneous economic returns to higher education. *American Sociological Review*, 75:273–302, 2010.

M. Browning and J. Carro. Heterogeneity and microeconometrics modeling. In R. Blundell, W. Newey, and T. Persson, editors, *Advances in Economics and Econometrics*, volume 3, pages 47–74. Cambridge University Press, 2007.

X. Cheng, F. Schorfheide, and P. Shao. Clustering for multi-dimensional heterogeneity. Working paper, 2019.

D. Chetverikov, B. Larsen, and C. Palmer. IV quantile regression for group-level treatments, with an application to the distributional effects of trade. *Econometrica*, 84:809–833, 2016.

J. L. Coles, N. D. Daniel, and L. Naveen. Managerial incentives and risk-taking. *Journal of Financial Economics*, 79:431–468, 2006.

M. Cytrynbaum. Blocked clusterwise regression. Working paper, 2020.

Y. Dong and A. Lewbel. Nonparametric identification of a binary random factor in cross section data. *Journal of Econometrics*, 163:163–171, 2011.

R. Duchin, J. G. Matsusaka, and O. Ozbas. When are outside directors effective? *Journal of Financial Economics*, 96:195–214, 2010.

A. Dzemski and R. Okui. Confidence set for group membership. Working papers, 2021.

W. Feller. *An Introduction to Probability Theory and Its Applications*, volume 2. John Wiley & Sons, 1991.

A. F. Galvao. Quantile regression for dynamic panel data with fixed effects. *Journal of Econometrics*, 164:142–157, 2011.

A. F. Galvao and K. Kato. Smoothed quantile regression for panel data. *Journal of Econometrics*, 193:92–112, 2016.

A. F. Galvao and G. Montes-Rojas. On bootstrap inference for quantile regression panel data: A monte carlo study. *Econometrics*, 3:654–666, 2015.

A. F. Galvao, T. Juhl, G. Montes-Rojas, and J. Olmo. Testing Slope Homogeneity in Quantile Regression Panel Data with an Application to the Cross-Section of Stock Returns. *Journal of Financial Econometrics*, 16:211–243, 2017.

A. F. Galvao, J. Gu, and S. Volgushev. On the unbiased asymptotic normality of quantile regression with fixed effects. *Journal of Econometrics*, 218:178–215, 2020.

A. F. Galvao, T. Parker, and Z. Xiao. Bootstrap inference for panel data quantile regression. memo, 2021.

J. Gu and S. Volgushev. Panel data quantile regression with grouped fixed effects. *Journal of Econometrics*, 213:68–91, 2019.

J. Hahn and H. R. Moon. Panel data models with finite number of multiple equilibria. *Econometric Theory*, 26:863–881, 2010.

K. Kato, A. F. Galvao, and G. V. Montes-Rojas. Asymptotics for panel quantile regression models with individual effects. *Journal of Econometrics*, 170:76–91, 2012.

Y. Ke, J. Li, and W. Zhang. Structure identification in panel data analysis. *The Annals of Statistics*, 44:1193–1233, 2016.

K. Knight. Limiting distributions for L_1 regression estimators under general conditions. *The Annals of Statistics*, 26:755–770, 1998.

R. Koenker. Quantile regression for longitudinal data. *Journal of Multivariate Analysis*, 91:74–89, 2004.

R. Koenker. *Quantile Regression*. Cambridge University Press, Cambridge, UK, 2005.

E. Krasnokutskaya, K. Song, and X. Tang. Estimating unobserved agent heterogeneity using pairwise comparisons. *Journal of Econometrics*, In Press, 2021.

C.-C. Lin and S. Ng. Estimation of panel data models with parameter heterogeneity when group membership is unknown. *Journal of Econometric Methods*, 1:42–55, 2012.

R. Liu, Z. Shang, Y. Zhang, and Q. Zhou. Identification and estimation in panel models with over-specified number of groups. *Journal of Econometrics*, 215:574–590, 2020.

K. Miao, L. Su, and W. Wang. Panel threshold regressions with latent group structures. *Journal of Econometrics*, 214:451–481, 2020.

T. Mitton. A cross-firm analysis of the impact of corporate governance on the East Asian financial crisis. *Journal of Financial Economics*, 64:215–241, 2002.

S. Ng and G. McLachlan. Mixture models for clustering multilevel growth trajectories. *Computational Statistics & Data Analysis*, 71:43–51, 2014.

R. Okui and W. Wang. Heterogeneous structural breaks in panel data models. *Journal of Econometrics*, 220:447–473, 2021.

M. Peligrad. On the asymptotic normality of sequences of weak dependent random variables. *Journal of Theoretical Probability*, 9:703–715, 1996.

O. Rosen, W. Jiang, and M. Tanner. Mixtures of marginal models. *Biometrika*, 87:391–404, 2000.

L. Su and W. Wang. Identifying latent group structures in nonlinear panels. *Journal of Econometrics*, 220:272–295, 2021.

L. Su, Z. Shi, and P. C. B. Phillips. Identifying latent structures in panel data. *Econometrica*, 84: 2215–2264, 2016.

Y. Sun. Estimation and inference in panel strcutural models. Working paper, Department of Economics, UCSD, 2005.

M. Vogt and O. Linton. Classification of non-parametric regression functions in longitudinal data models. *Journal of the Royal Statistical Society: Series B*, 79:5–27, 2016.

S. Volgushev, S.-K. Chao, G. Cheng, et al. Distributed inference for quantile regression processes. *The Annals of Statistics*, 47:1634–1662, 2019.

W. Wang, P. C. B. Phillips, and L. Su. Homogeneity pursuit in panel data models: Theory and application. *Journal of Applied Econometrics*, 33:797–815, 2018.

J. Yoon and A. F. Galvao. Cluster robust covariance matrix estimation in panel quantile regression with individual fixed effects. *Quantitative Economics*, 11:579–608, 2020.

Y. Zhang, H. J. Wang, and Z. Zhu. Quantile-regression-based clustering for panel data. *Journal of Econometrics*, 213:54–67, 2019a.

Y. Zhang, H. J. Wang, and Z. Zhu. Supplement to 'quantile-regression-based clustering for panel data'. *Journal of Econometrics Supplemental Material*, 213:54–67, 2019b.

E. Zwick and J. Mahon. Tax policy and heterogeneous investment behavior. *American Economic Review*, 107:217–48, 2017.